

Equipping Black-Box Policies with Model-Based Advice for Stable Nonlinear Control

Tongxin Li¹, Ruixiao Yang², Guannan Qu³, Yiheng Lin¹, Steven Low¹, and Adam Wierman¹

¹California Institute of Technology

²Tsinghua University

³Carnegie Mellon University

June 6, 2022

Abstract

Machine-learned black-box policies are ubiquitous for nonlinear control problems. Meanwhile, crude model information is often available for these problems from, e.g., linear approximations of nonlinear dynamics. We study the problem of equipping a black-box control policy with model-based advice for nonlinear control on a single trajectory. We first show a general negative result that a naive convex combination of a black-box policy and a linear model-based policy can lead to instability, even if the two policies are both stabilizing. We then propose an *adaptive λ -confident policy*, with a coefficient λ indicating the confidence in a black-box policy, and prove its stability. With bounded nonlinearity, in addition, we show that the adaptive λ -confident policy achieves a bounded competitive ratio when a black-box policy is near-optimal. Finally, we propose an online learning approach to implement the adaptive λ -confident policy and verify its efficacy in case studies about the CartPole problem and a real-world electric vehicle (EV) charging problem with data bias due to COVID-19.

Keywords— Black-box policy, stability, nonlinear control, EV charging affected by COVID-19

1 Introduction

Deep neural network (DNN)-based control methods such as deep reinforcement learning/imitation learning have attracted great interests due to the success on a wide range of control tasks such as humanoid locomotion [1], playing Atari [2] and 3D racing games [3]. These methods are typically model-free and are capable of learning policies and value functions for complex control tasks directly from raw data. In real-world applications such as autonomous driving, it is impractical to dynamically update the already-deployed policy. In those cases, pre-trained black-box policies are applied. Those partially-optimized solutions on the one hand can sometimes be optimal or near-optimal, but on the other hand can be arbitrarily poor in cases where there is unexpected environmental behavior due to, e.g., sample inefficiency [4], reward sparsity [5], mode collapse [6], high variability of policy gradient [7, 8], or biased training data [9]. This uncertainty raises significant concerns about applications of these tools in safety-critical settings. Meanwhile, for many real-world control problems, crude information about system models exists, e.g., linear approximations of their state transition dynamics [10, 11]. Such information can be useful in providing model-based advice to the machine-learned policies.

To represent such situations, in this paper we consider the following infinite-horizon dynamical system consisting of a *known* affine part, used for model-based advice, and an *unknown* nonlinear

residual function, which is (implicitly) used in developing machine-learned (DNN-based) policies:

$$x_{t+1} = \underbrace{Ax_t + Bu_t}_{\text{Known affine part}} + \underbrace{f_t(x_t, u_t)}_{\text{Unknown nonlinear residual}}, \quad \text{for } t = 0, \dots, \infty, \quad (1)$$

where $x_t \in \mathbb{R}^n$ and $u_t \in \mathbb{R}^m$ are the system state and the action selected by a controller at time t ; A and B are coefficient matrices in the affine part of the system dynamics. Besides the linear components, the system also has a state and action-dependent nonlinear residual $f_t : \mathbb{R}^n \times \mathbb{R}^m \rightarrow \mathbb{R}^n$ at each time $t \geq 0$, representing the modelling error. The matrices A and B are fixed and known coefficients in the linear approximation of the true dynamics (1).

Given the affine part of the dynamics (1), it is possible to construct a model-based feedback controller $\bar{\pi}$, e.g., a linear quadratic regulator or an \mathcal{H}_∞ controller. Compared with a DNN-based policy $\hat{\pi}(x_t)$, the induced linear controller often has a worse performance on average due to the model bias, but becomes more stable in an adversarial setting. In other words, a DNN-based policy can be as good as an optimal policy in domains where accurate training data has been collected, but can perform *sub-optimally* in other situations; while a policy based on a linearized system is *stabilizing*, so that it has a guaranteed worst-case performance with bounded system perturbations, but can lose out on performance to DNN-based policies in non-adversarial situations. We illustrate this trade-off for the CartPole problem (see Example 1 in Appendix 1) in Figure 1. The figure shows a pre-trained TRPO [12, 13] agent and an ARS [14] agent achieve lower costs when the initial angle of the pole is small; but become less stable when the initial angle increases. Using the affine part of the nonlinear dynamics, a linear quadratic regulator achieves better performance when the initial angle becomes large. Motivated by this trade-off, we ask the following question in this paper:

Can we equip a sub-optimal machine-learned policy $\hat{\pi}$ with stability guarantees for the nonlinear system (1) by utilizing model-based advice from the known, affine part?

Traditionally, switching between different control policies has been investigated for linear systems [15, 16]. All candidate policies need to be linear and therefore can be represented by their Youla–Kucera parametrizations (or Q-parameterizations). When a policy is a black-box machine-learned policy modeled by a DNN that may be nonlinear, how to combine or switch between the policies remains an open problem that is made challenging by the fact that the model-free policy typically has no theoretical guarantees associated with its performance. On the one hand, a model-free policy works well on average but, on the other hand, model-based advice stabilizes the system in extreme cases.

Contributions. In this work we propose a novel, adaptive policy that combines model-based advice with a black-box machine-learned controller to guarantee stability while retaining the performance of the machine-learned controller when it performs well. In particular, we consider a nonlinear control problem whose dynamics is given in (1), where we emphasize that the unknown nonlinear residual function $f_t(x_t, u_t)$ is time-varying and depends not only on the state x_t but also the action u_t at each time t . Our first result is a negative result (Theorem 1) showing that a naive convex combination of a black-box model-free policy with model-based advice can lead to instability, even if both policies are stabilizing individually. This negative result highlights the challenges associated with combining model-based and model-free approaches.

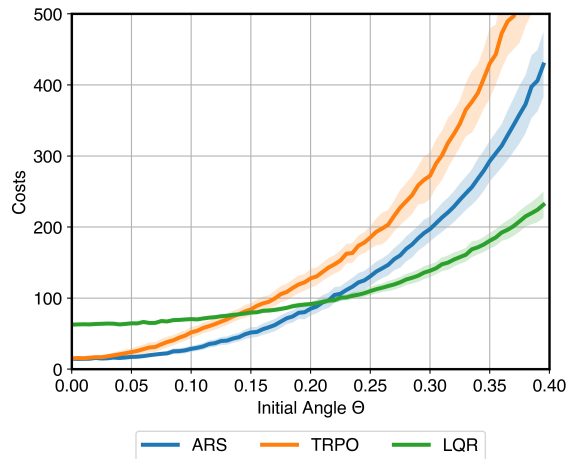


Figure 1: Costs of pre-trained TRPO and ARS agents and an LQR when the initial pole angle θ (unit: radians) varies.

Next, we present a general policy that adaptively combines a model-free black-box policy with model-based advice (Algorithm 1). We assume that the model-free policy has some consistency error ε , compared with the optimal policy and that the residual functions ($f_t : t \geq 0$) are Lipschitz continuous with a Lipschitz constant $C_\ell > 0$. Instead of employing a hard-switching between policies, we introduce a time-varying *confidence coefficient* λ_t that only decays and switches a black-box model-free policy into a stabilizing model-based policy in a smooth way during operation as needed to ensure stabilization. The sequence of confidence coefficients converges to $\lambda \in [0, 1]$. Our main result is the following theorem, which establishes a trade-off between competitiveness (Theorem 3) and stability (Theorem 2) of this adaptive algorithm.

Theorem (Informal). *With system assumptions (Assumption 1, 2 and an upper bound on C_ℓ), the adaptive λ -confident policy (Algorithm 1) has the following properties: (a) the policy is exponentially stabilizing whose decay rate increases when λ decreases; and (b) when the consistency error ε is small, the competitive ratio of the policy satisfies*

$$\text{CR}(\varepsilon) = (1 - \lambda) \times \underbrace{O(\overline{\text{CR}}_{\text{model}})}_{\text{Model-based bound}} + \underbrace{O(1/(1 - O(\varepsilon)))}_{\text{Model-free error}} + \underbrace{O(C_\ell \|x_0\|_2)}_{\text{Nonlinear dynamics error}}. \quad (2)$$

The theorem shows that the adaptive λ -confident policy is guaranteed to be stable. Furthermore, if the black-box policy is close to an optimal control policy (in the sense that the consistency error ε is small), then the adaptive λ -confident policy has a bounded competitive ratio that consists of three components. The first one is a bound inherited from a model-based policy; the second term depends on the sub-optimality gap between a black-box policy and an optimal policy; and the last term encapsulates the loss induced by switching from a policy to another and it scales with the ℓ_2 norm of an initial state x_0 and the nonlinear residuals (depending on the Lipschitz constant C_ℓ).

Our results imply an interesting trade-off between stability and sub-optimality, in the sense that if λ is smaller, it is guaranteed to stabilize with a higher rate and if λ becomes larger, it is able to have a smaller competitive ratio bound when provided with a high-quality black-box policy. Different from the linear case, where a cost characterization lemma can be directly applied to bound the difference between the policy costs and optimal costs in terms of the difference between their actions [17], for the case of nonlinear dynamics (1), we introduce an auxiliary linear problem to derive an upper bound on the dynamic regret, whose value can be decomposed into a quadratic term and a term induced by the nonlinearity. The first term can be bounded via a generalized characterization lemma and becomes the *model-based bound* and *model-free error* in (2). The second term becomes a *nonlinear dynamics error* via a novel sensitivity analysis of an optimal nonlinear policy based on its Bellman equation. Finally, we use the CartPole problem to demonstrate the efficacy of the adaptive λ -confident policy.

Related work. Our work is related to a variety of classical and learning-based policies for control and reinforcement learning (RL) problems that focus on combining model-based and model-free approaches.

Combination of model-based information with model-free methods. Our paper adds to the recent literature seeking to combine model-free and model-based policies for online control. Some prominent recent papers with this goal include the following. First, in [18], Q-learning is connected with model predictive control (MPC) whose constraints are Q-functions encapsulating the state transition information. Second, MPC methods with penalty terms learned by model-free algorithms are considered in [19]. Third, deep neural network dynamics models are used to initialize a model-free learner to improve the sample efficiency while maintaining the high task-specific performance [20]. Next, using this idea, the authors of [11] consider a more concrete dynamical system $x_{t+1} = Ax_t + Bu_t + f(x_t)$ (similar to the dynamics in (1) considered in this work) where f is a state-dependent function and they show that a model-based initialization of a model-free policy is guaranteed to converge to a near-optimal linear controller. Another approach uses an \mathcal{H}_∞ controller integrated into model-free RL algorithms for variance reduction [7]. Finally, the model-based value expansion is proposed

in [21] as a method to incorporate learned dynamics models in model-free RL algorithms. Broadly, despite many heuristic combinations of model-free and model-based policies demonstrating empirical improvements, there are few theoretical results explaining and verifying the success of the combination of model-free and model-based methods for control tasks. Our work contributes to this goal.

Combining stabilizing linear controllers. The proposed algorithm in this work combines existing controllers and so is related to the literature of combining stabilizing linear controllers. A prominent work in this area is [15], which shows that with proper controller realizations, switching between a family of stabilizing controllers uniformly exponentially stabilizes a linear time-invariant (LTI) system. Similar results are given in [16]. The techniques applied in [16, 15] use the fact that all the stabilizing controllers can be expressed using the Youla parameterization. Different from the classical results of switching between or combining stabilizing controllers, in this work, we generalize the idea to the combination of a linear model-based policy and a model-free policy, that can be either linear or nonlinear.

Learning-augmented online problems. Recently, the idea of augmenting robust/competitive online algorithms with machine-learned advice has attracted attention in online problems in settings like online caching [22], ski-rental [23, 24], smoothed online convex optimization [25, 26] and linear quadratic control [17]. In many of these learning-augmented online algorithms, a convex combination of machine-learned (untrusted) predictions and robust decisions is involved. For instance, in [17], competitive ratio upper bounds of a λ -confident policy are given for a linear quadratic control problem. The policy $\lambda\pi_{\text{MPC}} + (1 - \lambda)\pi_{\text{LQR}}$ combines linearly a linear quadratic regulator π_{LQR} and an MPC policy π_{MPC} with machine-learned predictions where $\lambda \in [0, 1]$ measures the confidence of the machine-learned predictions. To this point, no results on learning-augmented controllers for nonlinear control exist. In this work, we focus on the case of nonlinear dynamics and show a general negativity result (Theorem 1) such that a simple convex combination between two policies can lead to unstable outputs and then proceed to provide a new approach that yields positive results.

	Setting	Known	Unknown	(Partial) Assumption(s)	Objective
[27]	Episodic	h	f	$h, f \in \mathcal{C}^{0,1}$	Safe exploration
[7]	Episodic	f^{known}	f^{unknown}	$\ \hat{\pi} - \bar{\pi}\ _2 \leq C_\pi$ Stabilizable f^{known}	Lyapunov stability
[10]	Episodic	A, B	$g_t(x)$	Hurwitz A	Input-output stability
[11]	Episodic	A, B	$f(x)$	$f \in \mathcal{C}^{0,1}$, Stabilizable A, B	Lyapunov stability
[28, 29, 30]	Episodic		(C)MDP	Feasible baseline [28]	Safety and stability
This work	1-trajectory	A, B	$f_t(x, u)$	$f_t \in \mathcal{C}^{0,1}$, Stabilizable A, B	Stability, CR bound

Stability-certified RL. Another highly related line of work is the recent research on developing safe RL with stability guarantees. In [27], Lyapunov analysis is applied to guarantee the stability of a model-based RL policy. If an \mathcal{H}_∞ controller $\hat{\pi}_{\mathcal{H}_\infty}$ is close enough to a model-free deep RL policy $\bar{\pi}_{\text{RL}}$, by combining the two policies linearly $\lambda\hat{\pi}_{\mathcal{H}_\infty} + (1 - \lambda)\bar{\pi}_{\text{RL}}$ at each time in each training episode, asymptotic stability and forward invariance can be guaranteed using Lyapunov analysis but the convergence rate is not provided [7]. In practice, [7] uses an empirical approach to choose a time-varying factor λ according to the temporal difference error. Robust model predictive control (MPC) is combined with deep RL to ensure safety and stability [30]. Using regulated policy gradient, input-output stability is guaranteed for a continuous nonlinear control model $f_t(x(t)) = Ax(t) + Bu(t) + g_t(x(t))$ [10]. In those works, a common assumption needs to be made is the ability to access and update the deep RL policy during the episodic training steps. Moreover, in the state-of-the-art results, the stability guarantees are proven, either considering an aforementioned episodic setting when the black-box policy can be improved or customized [27, 10], or assuming a small and bounded output distance between a black-box policy and a stabilizing policy for any input states to construct a Lyapunov equation [7], which is less realistic. Stability guarantees under different model assumptions such as (constrained)

MDPs have been studied [28, 29, 30]. Different from the existing literature, the result presented in this work is unique and novel in the sense that we consider stability and sub-optimality guarantee for black-box deep policies in a single trajectory such that we can neither learn from the environments nor update the deep RL policy through extensive training steps. Denote by $\mathcal{C}^{0,1}$ the class of Lipschitz continuous functions (with domains, ranges and norms specified according to the contexts), the related results are summarized in the table above.

2 Background and Model

We consider the following infinite-horizon quadratic control problem with nonlinear dynamics:

$$\min_{(u_t: t \geq 0)} \sum_{t=0}^{\infty} x_t^\top Q x_t + u_t^\top R u_t, \text{ subject to (1)} \quad (3)$$

where in the problem $Q, R \succ 0$ are $n \times n$ and $m \times m$ positive definite matrices and each $f_t : \mathbb{R}^n \times \mathbb{R}^m \rightarrow \mathbb{R}^n$ in (1) is an unknown nonlinear function representing state and action-dependent perturbations. An initial state x_0 is fixed. We use the following assumptions throughout this paper. Our first assumption is the Lipschitz continuity assumption on the residual functions and it is standard [11]. Note that $\|\cdot\|$ denotes the Euclidean norm throughout the paper.

Assumption 1 (Lipschitz continuity). *The function $f_t : \mathbb{R}^n \times \mathbb{R}^m \rightarrow \mathbb{R}^n$ is Lipschitz continuous for any $t \geq 0$, i.e., there is a constant $C_\ell \geq 0$ such that $\|f_t(x) - f_t(y)\| \leq C_\ell \|x - y\|$ for any $x, y \in \mathbb{R}^n$ and $t \geq 0$. Moreover, $f(0) = 0$.*

Next, we make a standard assumption on the system stability and cost function [31, 32].

Assumption 2 (System stabilizability and costs). *The pair of matrices (A, B) is stabilizable, i.e., there exists a real matrix K such that the spectral radius $\rho(A - BK) < 1$. We assume $Q, R \succeq \sigma I$. Furthermore, denote $\kappa := \max\{2, \|A\|, \|B\|\}$.*

In summary, our control agent is provided with a black-box policy $\hat{\pi}$ and system parameters A, B, Q, R . The goal is to utilize $\hat{\pi}$ and system information to minimize the quadratic costs in (3), without knowing nonlinear residuals ($f_t : t \geq 0$). Next, we present our policy assumptions.

Model-based advice. In many real-world applications, linear approximations of the true nonlinear system dynamics are known, i.e., the known affine part of (1) is available to construct a stabilizing policy $\bar{\pi}$. To construct $\bar{\pi}$, the assumption that (A, B) is stabilizable implies that the following discrete algebraic Riccati equation (DARE) has a unique semi-positive definite solution P that stabilizes the closed-loop system [33]:

$$P = Q + A^\top P A - A^\top P B (R + B^\top P B)^{-1} B^\top P A. \quad (4)$$

Given P , define $K := (R + B^\top P B)^{-1} B^\top P A$. The closed-loop system matrix $F := A - BK$ must have a spectral radius $\rho(F)$ less than 1. Therefore, the Gelfand's formula implies that there must exist a constant $C_F > 0$, $\rho \in (0, 1)$ such that $\|F^t\| \leq C_F \rho^t$, for any $t \geq 0$. The model-based advice considered in this work is then defined as a sequence of actions ($u_t : t \geq 0$) provided by a linear quadratic regulator (LQR) such that $u_t = \bar{\pi}(x_t) = -Kx_t$.

Black-box model-free policy. To solve the nonlinear control problem in (3), we take advantage of both model-free and model-based approaches. We assume a pre-trained model-free policy, whose policy is denoted by $\hat{\pi} : \mathbb{R}^n \rightarrow \mathbb{R}^m$, is provided beforehand. The model-free policy is regarded as a "black box", whose detail is not the major focus in this paper. The only way we interact with it is to obtain a suggested action $\hat{u}_t = \hat{\pi}(x_t)$ when feeding into it the current system state x_t . The

performance of the model-free policy is not guaranteed and it can make some error, characterized by the following definition, which compares $\hat{\pi}$ against a clairvoyant optimal controller π_t^* knowing the nonlinear residual perturbations in hindsight:

Definition 1 (ε -consistency). *A policy $\pi : \mathbb{R}^n \rightarrow \mathbb{R}^m$ is called ε -consistent if there exists $\varepsilon > 0$ such that for any $x \in \mathbb{R}^n$ and $t \geq 0$, $\|\pi(x) - \pi_t^*(x)\| \leq \varepsilon\|x\|$ where π_t^* denotes an optimal policy at time t knowing all the nonlinear residual perturbations ($f_t : t \geq 0$) in hindsight and ε is called a consistency error.*

The parameter ε measures the difference between the action given by the oracle policy $\hat{\pi}$ and the optimal action given the state x . There is no guarantee that ε is small. With prior knowledge of the nonlinearity of system gained from data, the sub-optimal model-free policy $\hat{\pi}$ suffers a consistency error $\varepsilon > 0$, which can be either small if the black-box policy is trained by unbiased data; or high because of the high variability issue for policy gradient deep RL algorithms [7, 8] and distribution shifts of the environments. In these cases, the error $\varepsilon > 0$ can be large. In this paper, we augment a black-box model-free policy with stability guarantees using the idea of adaptively switching it to a model-based stabilizing policy $\bar{\pi}$, which often exists provided with exact or estimates of system parameters A, B, Q and R . The linear stabilizing policy is conservative and highly sub-optimal as it is neither designed based on the exact nonlinear model nor interacts with the environment like the training of $\hat{\pi}$ potentially does.

Performance metrics. Our goal is to ensure stabilization of states while also providing good performance, as measured by the competitive ratio. Formally, a policy π is (asymptotically) *stabilizing* if it induces a sequence of states ($x_t : t \geq 0$) such that $\|x_t\| \rightarrow 0$ as $t \rightarrow \infty$. If there exist $C > 0$ and $0 \leq \gamma < 1$ such that $\|x_t\| \leq C\gamma^t\|x_0\|$ for any $t \geq 0$, the corresponding policy is said to be exponentially stabilizing. To define the competitive ratio, let OPT be the offline optimal cost of (3) induced by optimal control policies ($\pi_t^* : t \geq 0$) when the nonlinear residual functions ($f_t : t \geq 0$) are known in hindsight, and ALG be the cost achieved by an online policy. Throughout this paper we assume $\text{OPT} > 0$. We formally define the competitive ratio as follows.

Definition 2. *Given a policy, the corresponding competitive ratio, denoted by CR, is defined as the smallest constant $C \geq 1$ such that $\text{ALG} \leq C \cdot \text{OPT}$ for fixed A, B, Q, R satisfying Assumption 2 and any adversarially chosen residual functions ($f_t : t \geq 0$) satisfying Assumption 1.*

3 Warm-up: A Naive Convex Combination

The main results in this work focus on augmenting a black-box policy $\hat{\pi}$ with stability guarantees while minimizing the quadratic costs in (3), provided with linear system parameters A, B, Q, R of a nonlinear system. Before proceeding to our policy, to highlight the challenge of combining model-based advice with model-free policies in this setting we first consider a simple strategy for combining the two via a convex combination. This is an approach that has been proposed and studied previously, e.g., [7, 17]. However, we show that it can be problematic in that it can yield an unstable policy even when the two policies are stabilizing individually. Then, in Section 4, we propose an approach that overcomes this challenge.

A natural approach for incorporating model-based advice is a convex combination of a model-based control policy $\bar{\pi}$ and a black-box model-free policy $\hat{\pi}$. The combined policy generates an action $u_t = \lambda\hat{\pi}(x_t) + (1 - \lambda)\bar{\pi}(x_t)$ given a state x_t at each time, where $\lambda \in [0, 1]$. The coefficient λ determines a confidence level such that if λ is larger, we trust the black-box policy more and vice versa. In the following, however, we highlight that, in general, the convex combination of two policies can yield an unstable policy, even if the two policies are stabilizing, with a proof in Appendix D.

Theorem 1. *Assume B is an $n \times n$ full-rank matrix with $n > 1$. For any $\lambda \in (0, 1)$ and any linear controller K_1 satisfying $A - BK_1 \neq 0$, there exists a linear controller K_2 that stabilizes the*

system such that their convex combination $\lambda K_2 + (1 - \lambda)K_1$ is unstable, i.e., the spectral radius $\rho(A - B(\lambda K_2 + (1 - \lambda)K_1)) > 1$.

Theorem 1 brings up an issue with the strategy of combining a stabilizing policy with a model-free policy. Even if both the model-based and model-free policies are stabilizing, the combined controller can lead to unstable state outputs. In general, the space of stabilizing linear controllers $\{K \in \mathbb{R}^{n \times m} : K \text{ is stabilizing}\}$ is nonconvex [34]. The result in Theorem 1 is a stronger statement. It implies that for any arbitrarily chosen linear policy K_1 and a coefficient $\lambda \in (0, 1)$, we can always adversarially select a second policy K_2 such that their convex combination leads to an unstable system. It is worth emphasizing that the second policy does not necessarily have to be a complicated nonlinear policy. Indeed, in our proof, we construct a linear policy K_2 to derive the conclusion. In our problem, the second policy K_2 is assumed to be a black-box policy $\hat{\pi}$ potentially parameterized by a deep neural network, yielding much more uncertainty on a similar convex combination. As a result, we must be careful when combining policies together.

Note that the idea of applying a convex combination of an RL policy and a control-theoretic policy linearly is not a new approach and similar policy combinations have been proposed in previous studies [7, 17]. However, in those results, either the model-free policy is required to satisfy specific structures [17] or to be close enough to the stabilizing policy [7] to be combined. In [17], a learning-augmented policy is combined with a linear quadratic regulator, but the learning-augmented policy has a specific form and it is not a black-box policy. In [7], a deep RL policy $\hat{\pi}$ is combined with an \mathcal{H}^∞ controller $\bar{\pi}$ and they need to satisfy that for any state $x \in \mathbb{R}^n$, $\|\hat{\pi}(x) - \bar{\pi}(x)\| \leq C_\pi$ for some $C_\pi > 0$. However, it is possible that when the state norm $\|x\|$ becomes large, the two policies in practice behave entirely differently. Moreover, it is hard to justify the benefit of combining two policies, conditioned on the fact that they are already similar. Given that those assumptions are often not satisfied or hard to be verified in practice, we need another approach to guarantee worst-case stability when the black-box policy is biased and in addition ensure sub-optimality if the black-box policy works well.

4 Adaptive λ -confident Control

Motivated by the challenge highlighted in the previous section, we now propose a general framework that adaptively selects a sequence of monotonically decreasing confidence coefficients ($\lambda_t : t \geq 0$) in order to switch between black-box and stabilizing model-based policies. We show that it is possible to guarantee a bounded competitive ratio when the black-box policy works well, i.e., it has a small consistency error ε , and guarantee stability in cases when the black-box policy performs poorly.

The adaptive λ -confident policy introduced in Algorithm 1 involves an input coefficient λ' at each time. The value of λ_t can either be λ_{t-1} decreased by a fixed step size α , or a variable learned from known system parameters in (3) combined with observations of previous states and actions. In Section 5.1, we consider an online learning approach to generate a value of λ' at each time t , but it is worth emphasizing that the adaptive policy in Algorithm 1 and its theoretical guarantees in Section 4.1 do not require specifying a detailed construction of λ' .

The adaptive policy differs from the naive convex combination that has been discussed in Section 3 in that it adopts a sequence of time-varying and monotonically decreasing coefficients ($\lambda_t : t \geq 0$) to combine a black-box policy and a model-based stabilizing policy, where the former policy is adaptively switched to the later one. The coefficient λ_t converges to $\lim_{t \rightarrow \infty} \lambda_t = \lambda$, where the limit λ can be a positive value, if the state converges to a target equilibrium ($\mathbf{0}$ under our model assumptions) before λ_t decreases to zero. This helps stabilize the system under assumptions on the Lipschitz constant C_ℓ of unknown nonlinear residual functions and if the black-box policy is near-optimal, a bounded competitive ratio is guaranteed, as we show in the next section.

4.1 Theoretical guarantees

Algorithm 1: Adaptive λ -confident

Data: System parameters A, B, Q, R, α
for $t \geq 0$ **do**
 if $t = 0$ **then** Initialize $\lambda_0 \leftarrow 1$
 if $\|x_t\| = 0$ **then** $\lambda_t \leftarrow \lambda_t$
 else
 Obtain a coefficient λ'
 \triangleright Online learning (Eq. (6))
 if $\lambda' > 0$ and $\lambda_{t-1} > \alpha$ **then**
 $\lambda_t \leftarrow \min\{\lambda', \lambda_{t-1} - \alpha\}$
 else $\lambda_t \leftarrow 0$
 end
 Generate an action
 $u_t = \lambda_t \hat{\pi}(x_t) + (1 - \lambda_t) \bar{\pi}(x_t)$
 Update state according to (1)
end

are the known system parameters in (3), P has been defined in the Riccati equation (4); $C_F > 0$ and $\rho \in (0, 1)$ are constants such that $\|F^t\| \leq C_F \rho^t$, for any $t \geq 0$ as defined in Section 2; C_ℓ is the Lipschitz constant in Assumption 1; $\varepsilon > 0$ is the consistency error in Definition 1; Finally, $C_a^{\text{sys}}, C_b^{\text{sys}}, C_c^{\text{sys}} > 0$ are constants that only depend on the known system parameters in (3) and they are listed in Appendix B.

Given the above notation, the theorem below guarantees stability of the adaptive λ -confident policy.

Theorem 2. Suppose the Lipschitz constant C_ℓ satisfies $C_\ell < \frac{1-\rho}{C_F(1+\|K\|)}$. The adaptive λ -confident policy (Algorithm 1) is an exponentially stabilizing policy such that $\|x_t\| = O((\mu/\gamma)^{t_0} \gamma^t) \|x_0\|$.

For Theorem 2 to hold such that $\gamma < 1$, the Lipschitz constant C_ℓ needs to have an upper bound $\frac{1-\rho}{C_F(1+\|K\|)}$ where $C_F > 0$ and $\rho \in (0, 1)$ are constants such that $\|F^t\| \leq C_F \rho^t$, for any $t \geq 0$. Since A and B are stabilizable, such C_F and ρ exist. The upper bound only depends on the known system parameters A, B, Q and R . A small enough Lipschitz constant is required to guarantee stability. For instance, in [11], convergence exponentially to the equilibrium state is guaranteed when the Lipschitz constant satisfies $C_\ell = O\left(\frac{\sigma^2(1-\rho)^8}{\kappa^9 C_F^{15}}\right)$.

Competitiveness. Define a constant $\overline{\text{CR}}_{\text{model}} := 2\kappa \left(\frac{C_F \|P\|}{1-\rho}\right)^2 / \sigma$. The theorem below implies that when the model-free policy error ε and the Lipschitz constant C_ℓ of the residual functions are small enough, Algorithm 1 is competitive.

Theorem 3. Suppose the Lipschitz constant satisfies $C_\ell < \min\{1, C_a^{\text{sys}}, C_c^{\text{sys}}\}$. When the consistency error satisfies $\varepsilon < \min\left\{\frac{\sigma}{2\|H\|}, \frac{1/C_F - C_a^{\text{sys}} C_\ell}{C_\ell + \|B\|}\right\}$, the competitive ratio of the adaptive λ -confident policy (Algorithm 1) is bounded by

$$\text{CR}(\varepsilon) = (1 - \lambda) \overline{\text{CR}}_{\text{model}} + O\left(1 / \left(1 - \frac{2\|H\|}{\sigma} \varepsilon\right)\right) + O(C_\ell \|x_0\|).$$

Combining Theorem 2 and 3, our main results are proved when the Lipschitz constant satisfies $C_\ell < \min\left\{1, C_a^{\text{sys}}, C_c^{\text{sys}}, \frac{(1-\rho)}{C_F(1+\|K\|)}\right\}$. Theorem 2 and 3 have some interesting implications. First, if the selected time-varying confidence coefficients converge to a λ that is large, then we trust the black-box policy and use a higher weight in the per-step combination. This requires a slower decaying rate of λ_t to zero so as a trade-off, t_0 can be higher and this leads to a weaker stability result and

The theoretical guarantees we obtain are two-fold. First, we show that the adaptive λ -confident policy in Algorithm 1 is stabilizing, as stated in Theorem 2. Second, in addition to stability, we show that the policy has a bounded competitive ratio, if the black-box policy used has a small consistency error (Theorem 3). Note that if a black-box policy has a large consistency error ε , without using model-based advice, it can lead to instability and therefore possibly an unbounded competitive ratio.

Stability. Before presenting our results, we introduce some new notation for convenience. Denote by t_0 the smallest time index when $\lambda_t = 0$ or $x_t = \mathbf{0}$ and note that $\mathbf{0}$ is an equilibrium state. Denote by $\lambda = \lim_{t \rightarrow \infty} \lambda_t$. Since $(\lambda_t : t \geq 0)$ is a monotonically decreasing sequence and λ_t has a lower bound, t_0 and λ exist and are unique. Let $H := R + B^\top P B$. Define the parameters $\gamma := \rho + C_F C_\ell (1 + \|K\|)$ and $\mu := C_F (\varepsilon (C_\ell + \|B\|) + C_a^{\text{sys}} C_\ell)$ where A, B, Q, R

vice versa. In contrast, when the nonlinear dynamics in (1) becomes linear with unknown constant perturbations, [17] shows a trade-off between robustness and consistency, i.e., a universal competitive ratio bound holds, regardless the error of machine-learned predictions. Different from the linear case where a competitive ratio bound always exists and can be decomposed into terms parameterized by some confidence coefficient λ , for the nonlinear system dynamics (1), there are additional terms due to the nonlinearity of the system that can only be bounded if the consistency error ε is small. This highlights a fundamental difference between linear and nonlinear systems, where the latter is known to be more challenging. Proofs of Theorem 2 and 3 are provided in Appendix E and F.

5 Practical Implementation and Experiments

5.1 Learning confidence coefficients online

Our main results in the previous section are stated without specifying a sequence of confidence coefficients $(\lambda_t : t \geq 0)$ for the policy; however in the following we introduce an online learning approach to generate confidence coefficients based on observations of actions, states and known system parameters. The negative result in Theorem 1 highlights that the adaptive nature of the confidence coefficients in Algorithm 1 are crucial to ensuring stability. Naturally, learning the values of the confidence coefficients $(\lambda_t : t \geq 0)$ online can further improve performance.

In this section we propose an online learning approach based on a linear parameterization of a black-box model-free policy $\hat{\pi}_t(x) = -Kx - H^{-1}B^\top \sum_{\tau=t}^{\infty} (F^\top)^{t-\tau} P \hat{f}_\tau$ where $(\hat{f}_t : t \geq 0)$ are parameters representing estimates of the residual functions for a black-box policy. Note that when $\hat{f}_t = f_t^* := f_t(x_t^*, u_t^*)$ where x_t^* and u_t^* are optimal state and action at time t for an optimal policy, then the model-free policy is optimal. In general, a black-box model-free policy $\hat{\pi}$ can be nonlinear, the linear parameterization provides an example of how the time-varying confidence coefficients $(\lambda_t : t \geq 0)$ are selected and the idea can be extended to nonlinear parameterizations such as kernel methods.

Under the linear parameterization assumption, for linear dynamics, [17] shows that the optimal choice of λ_{t+1} that minimizes the gap between the policy cost and optimal cost for the t time steps is

$$\lambda_{t+1} = \left(\sum_{s=0}^t (\eta(f^*; s, t))^\top H (\eta(\hat{f}; s, t)) \right) / \left(\sum_{s=0}^t (\eta(\hat{f}; s, t))^\top H (\eta(\hat{f}; s, t)) \right), \quad (5)$$

where $\eta(f; s, t) := \sum_{\tau=s}^t (F^\top)^{\tau-s} P f_\tau$. Compared with a linear quadratic control problem, computing λ_t in (5) raises two problems. The first is different from a linear dynamical system where true perturbations can be observed, the optimal actions and states are unknown, making the computation of the term $\eta(f^*; s, t-1)$ impossible. The second issue is similar. Since the model-free policy is a black-box, we do not know the parameters $(\hat{f}_t : t \geq 0)$ exactly. Therefore, we use approximations to compute the terms $\eta(f^*; s, t)$ and $\eta(\hat{f}; s, t)$ in (5) and the linear parameterization and linear dynamics assumptions are used to derive the approximations respectively with details provided in Appendix B. Let $(BH^{-1})^\dagger$ denote the Moore–Penrose inverse of BH^{-1} . Combining (8) and (9) with (5) yields the following online-learning choice of a confidence coefficient $\lambda_t = \min \{\lambda', \lambda_{t-1} - \alpha\}$ where $\alpha > 0$ is a fixed step size and

$$\lambda' := \frac{\sum_{s=1}^{t-1} \left(\sum_{\tau=s}^{t-1} (F^\top)^{\tau-s} P (Ax_\tau + Bu_\tau - x_{\tau+1}) \right)^\top B (\hat{u}_s + Kx_s)}{\sum_{s=0}^{t-1} (\hat{u}_s + Kx_s)^\top (BH^{-1})^\dagger B (\hat{u}_s + Kx_s)} \quad (6)$$

based on the crude model information A, B, Q, R and previously observed states, model-free actions and policy actions. This online learning process provides a choice of the confidence coefficient in

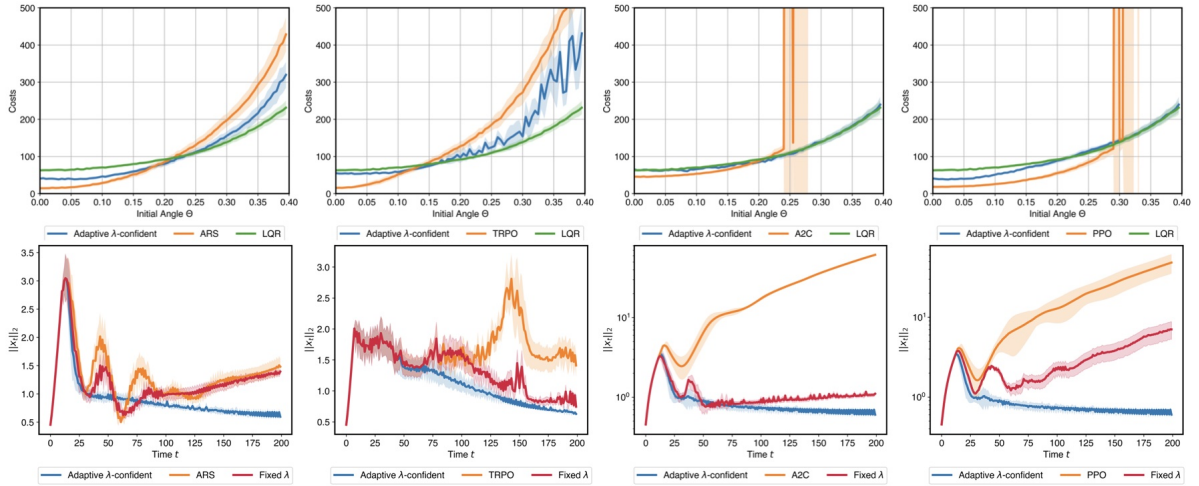


Figure 2: Top (*Competitiveness*): costs of pre-trained RL agents, an LQR and the adaptive policy when the initial pole angle θ (unit: radians) varies. Bottom (*stability*): convergence of $\|x_t\|$ in t with $\theta = 0.4$ for pre-trained RL agents, a naive combination (Section 3) using a fixed $\lambda = 0.8$ and the adaptive policy.

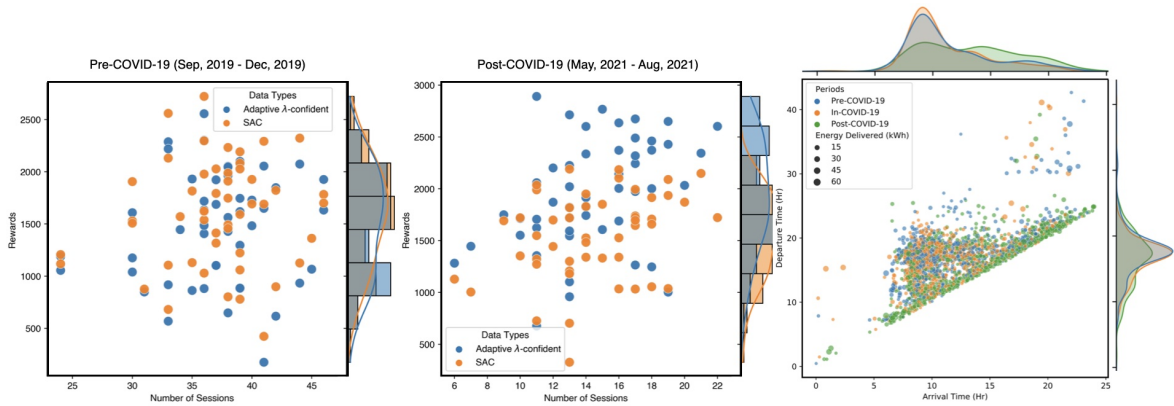


Figure 3: Left: total rewards of the adaptive policy and SAC for pre-COVID-19 days and post-COVID-19 days. Right: shift of data distributions due to the work-from-home policy.

Algorithm 1. It is worth noting that other approaches for generating λ_t exist, and our theoretical guarantees apply to any approach.

5.2 Experiments

To demonstrate the efficacy of the adaptive λ -confident policy (Algorithm 1), we first apply it to the CartPole OpenAI gym environment (CartPole-v1, Example 1 in Appendix A) [35].¹ Next, we apply it to an adaptive electric vehicle (EV) charging environment modeled by a real-world dataset [36].

The CartPole problem. We use the Stable-Baselines3 pre-trained agents [13] of A2C [37], ARS [14], PPO [1] and TRPO [12] as four candidate black-box policies. In Figure 2, the adaptive policy finds a trade-off between the pre-trained black-box policies and an LQR with crude model information (i.e., about 50% estimation error in the mass and length values). In particular, when θ increases, it stabilizes the state while the A2C and PPO policies become unstable when the initial angle θ is large.

¹The CartPole environment is modified so that quadratic costs are considered rather than discrete rewards.

Real-world adaptive EV charging. In the EV charging application, a SAC [38] agent is trained with data collected from a pre-COVID-19 period and tested on days before and after COVID-19. Due to a policy change (the work-from-home policy), the SAC agent becomes biased in the post-COVID-19 period (see the right sub-figure in Figure 3). With crude model information, the adaptive policy has rewards matching the SAC agent in the pre-COVID-19 period and significantly outperforms the SAC agent in the post-COVID-19 period with an average total award 1951.2 versus 1540.3 for SAC. Further details on the hyper-parameters and reward function are included in Appendix A.

6 Concluding Remarks

This work considers a novel combination of pre-trained black-box policies with model-based advice from crude model information. A general adaptive policy is proposed, with theoretical guarantees on both stability and sub-optimality. The effectiveness of the adaptive policy is validated empirically. We believe that the results presented lead to an important first step towards improving the practicality of existing DNN-based algorithms when using them as black-boxes in nonlinear real-world control problems. Exploring other forms of model-based advice theoretically, and verifying practically other implementations to learn the confidence coefficients online are interesting future directions.

References

- [1] John Schulman, Filip Wolski, Prafulla Dhariwal, Alec Radford, and Oleg Klimov. Proximal policy optimization algorithms. *arXiv preprint arXiv:1707.06347*, 2017.
- [2] Volodymyr Mnih, Koray Kavukcuoglu, David Silver, Alex Graves, Ioannis Antonoglou, Daan Wierstra, and Martin Riedmiller. Playing atari with deep reinforcement learning. *arXiv preprint arXiv:1312.5602*, 2013.
- [3] Stéphane Ross, Geoffrey Gordon, and Drew Bagnell. A reduction of imitation learning and structured prediction to no-regret online learning. In *Proceedings of the fourteenth international conference on artificial intelligence and statistics*, pages 627–635. JMLR Workshop and Conference Proceedings, 2011.
- [4] Matthew Botvinick, Sam Ritter, Jane X Wang, Zeb Kurth-Nelson, Charles Blundell, and Demis Hassabis. Reinforcement learning, fast and slow. *Trends in cognitive sciences*, 23(5):408–422, 2019.
- [5] Martin Riedmiller, Roland Hafner, Thomas Lampe, Michael Neunert, Jonas Degraeve, Tom Wiele, Vlad Mnih, Nicolas Heess, and Jost Tobias Springenberg. Learning by playing solving sparse reward tasks from scratch. In *International conference on machine learning*, pages 4344–4353. PMLR, 2018.
- [6] Allan Jabri, Kyle Hsu, Abhishek Gupta, Ben Eysenbach, Sergey Levine, and Chelsea Finn. Unsupervised curricula for visual meta-reinforcement learning. *Advances in Neural Information Processing Systems*, 32, 2019.
- [7] Richard Cheng, Abhinav Verma, Gabor Orosz, Swarat Chaudhuri, Yisong Yue, and Joel Burdick. Control regularization for reduced variance reinforcement learning. In *International Conference on Machine Learning*, pages 1141–1150. PMLR, 2019.
- [8] Benjamin Recht. A tour of reinforcement learning: The view from continuous control. *Annual Review of Control, Robotics, and Autonomous Systems*, 2:253–279, 2019.

- [9] Xueying Bai, Jian Guan, and Hongning Wang. A model-based reinforcement learning with adversarial training for online recommendation. *Advances in Neural Information Processing Systems*, 32, 2019.
- [10] Ming Jin and Javad Lavaei. Stability-certified reinforcement learning: A control-theoretic perspective. *IEEE Access*, 8:229086–229100, 2020.
- [11] Guannan Qu, Chenkai Yu, Steven Low, and Adam Wierman. Exploiting linear models for model-free nonlinear control: A provably convergent policy gradient approach. In *2021 60th IEEE Conference on Decision and Control (CDC)*, pages 6539–6546. IEEE, 2021.
- [12] John Schulman, Sergey Levine, Pieter Abbeel, Michael Jordan, and Philipp Moritz. Trust region policy optimization. In *International conference on machine learning*, pages 1889–1897. PMLR, 2015.
- [13] Antonin Raffin, Ashley Hill, Adam Gleave, Anssi Kanervisto, Maximilian Ernestus, and Noah Dormann. Stable-baselines3: Reliable reinforcement learning implementations. *Journal of Machine Learning Research*, 22(268):1–8, 2021.
- [14] Horia Mania, Aurelia Guy, and Benjamin Recht. Simple random search of static linear policies is competitive for reinforcement learning. *Advances in Neural Information Processing Systems*, 31, 2018.
- [15] Joao P Hespanha and A Stephen Morse. Switching between stabilizing controllers. *Automatica*, 38(11):1905–1917, 2002.
- [16] Henrik Niemann, Jakob Stoustrup, and Rune B Abrahamsen. Switching between multivariable controllers. *Optimal control applications and methods*, 25(2):51–66, 2004.
- [17] Tongxin Li, Ruixiao Yang, Guannan Qu, Guanya Shi, Chenkai Yu, Adam Wierman, and Steven Low. Robustness and consistency in linear quadratic control with untrusted predictions. *Proceedings of the ACM on Measurement and Analysis of Computing Systems*, 6(1):1–35, 2022.
- [18] V. Pong*, S. Gu*, M. Dalal, and S. Levine. Temporal difference models: Model-free deep rl for model-based control. In *6th International Conference on Learning Representations (ICLR)*, May 2018. *equal contribution.
- [19] Ugo Rosolia and Francesco Borrelli. Learning model predictive control for iterative tasks. a data-driven control framework. *IEEE Transactions on Automatic Control*, 63(7):1883–1896, 2017.
- [20] Anusha Nagabandi, Gregory Kahn, Ronald S Fearing, and Sergey Levine. Neural network dynamics for model-based deep reinforcement learning with model-free fine-tuning. In *2018 IEEE International Conference on Robotics and Automation (ICRA)*, pages 7559–7566. IEEE, 2018.
- [21] Vladimir Feinberg, Alvin Wan, Ion Stoica, Michael I Jordan, Joseph E Gonzalez, and Sergey Levine. Model-based value expansion for efficient model-free reinforcement learning. In *Proceedings of the 35th International Conference on Machine Learning (ICML 2018)*, 2018.
- [22] Thodoris Lykouris and Sergei Vassilvitskii. Competitive caching with machine learned advice. In *International Conference on Machine Learning*, pages 3296–3305. PMLR, 2018.
- [23] Manish Purohit, Zoya Svitkina, and Ravi Kumar. Improving online algorithms via ml predictions. In *Advances in Neural Information Processing Systems*, pages 9661–9670, 2018.

- [24] Alexander Wei and Fred Zhang. Optimal robustness-consistency trade-offs for learning-augmented online algorithms. *Advances in Neural Information Processing Systems*, 33:8042–8053, 2020.
- [25] Daan Rutten, Nico Christianson, Debankur Mukherjee, and Adam Wierman. Online optimization with untrusted predictions. *arXiv preprint arXiv:2202.03519*, 2022.
- [26] Nicolas Christianson, Tinashe Handina, and Adam Wierman. Chasing convex bodies and functions with black-box advice. In *Proceedings of COLT*, 2022.
- [27] Felix Berkenkamp, Matteo Turchetta, Angela Schoellig, and Andreas Krause. Safe model-based reinforcement learning with stability guarantees. *Advances in neural information processing systems*, 30, 2017.
- [28] Yinlam Chow, Ofir Nachum, Edgar Duenez-Guzman, and Mohammad Ghavamzadeh. A lyapunov-based approach to safe reinforcement learning. *Advances in neural information processing systems*, 31, 2018.
- [29] Theodore J Perkins and Andrew G Barto. Lyapunov design for safe reinforcement learning. *Journal of Machine Learning Research*, 3(Dec):803–832, 2002.
- [30] Mario Zanon and Sébastien Gros. Safe reinforcement learning using robust mpc. *IEEE Transactions on Automatic Control*, 66(8):3638–3652, 2020.
- [31] Horia Mania, Stephen Tu, and Benjamin Recht. Certainty equivalence is efficient for linear quadratic control. *Advances in Neural Information Processing Systems*, 32, 2019.
- [32] Sarah Dean, Horia Mania, Nikolai Matni, Benjamin Recht, and Stephen Tu. On the sample complexity of the linear quadratic regulator. *Foundations of Computational Mathematics*, 20(4):633–679, 2020.
- [33] William M Wonham. On a matrix riccati equation of stochastic control. *SIAM Journal on Control*, 6(4):681–697, 1968.
- [34] Yang Zheng, Luca Furieri, Antonis Papachristodoulou, Na Li, and Maryam Kamgarpour. On the equivalence of youla, system-level, and input–output parameterizations. *IEEE Transactions on Automatic Control*, 66(1):413–420, 2020.
- [35] Greg Brockman, Vicki Cheung, Ludwig Pettersson, Jonas Schneider, John Schulman, Jie Tang, and Wojciech Zaremba. Openai gym. *arXiv preprint arXiv:1606.01540*, 2016.
- [36] Zachary J Lee, Tongxin Li, and Steven H Low. Acn-data: Analysis and applications of an open ev charging dataset. In *Proceedings of the Tenth ACM International Conference on Future Energy Systems*, pages 139–149, 2019.
- [37] Volodymyr Mnih, Adria Puigdomenech Badia, Mehdi Mirza, Alex Graves, Timothy Lillicrap, Tim Harley, David Silver, and Koray Kavukcuoglu. Asynchronous methods for deep reinforcement learning. In *International conference on machine learning*, pages 1928–1937. PMLR, 2016.
- [38] Tuomas Haarnoja, Aurick Zhou, Pieter Abbeel, and Sergey Levine. Soft actor-critic: Off-policy maximum entropy deep reinforcement learning with a stochastic actor. In *International conference on machine learning*, pages 1861–1870. PMLR, 2018.
- [39] Chenkai Yu, Guanya Shi, Soon-Jo Chung, Yisong Yue, and Adam Wierman. Competitive control with delayed imperfect information. *arXiv preprint arXiv:2010.11637*, 2020.

A Experimental Setup and Supplementary Results

We describe the experimental settings and choices of hyper-parameters and reward/cost functions in the two applications.

Table 1: Hyper-parameters used in the CartPole problem.

Parameter	Value
Number of Monte Carlo Tests	10
Initial angle variation (in rad)	$\theta \pm 0.05$
Cost matrix Q	I
Cost matrix R	$[10^{-4}]$
Acceleration of gravity g (in m/s^2)	9.8
Pole mass m (in kg)	0.2 for LQR; 0.1 for real environment
Cart mass M (in kg)	2.0 for LQR; 1.0 for real environment
Pole length l (in m)	2
Duration τ (in second)	0.02
Force magnitude F	10
CPU	Intel® i7-8850H

A.1 The CartPole problem

Problem setting. The CartPole problem considered in the experiments is described by the following example.

Example 1 (The CartPole Problem). *In the CartPole problem, the goal of a controller is to stabilize the pole in the upright position. Neglecting friction, the dynamical equations of the CartPole problem are*

$$\ddot{\theta} = \frac{g \sin \theta + \cos \theta \left(\frac{-u - ml\dot{\theta}^2 \sin \theta}{m+M} \right)}{l \left(\frac{4}{3} - \frac{m \cos^2 \theta}{m+M} \right)}, \quad \ddot{y} = \frac{u + ml \left(\dot{\theta}^2 \sin \theta - \ddot{\theta} \cos \theta \right)}{m + M}$$

where u is the input force; θ is the angle between the pole and the vertical line; y is the location of the pole; g is the gravitational acceleration; l is the pole length; m is the pole mass; and M is the cart mass. Taking $\sin \theta \approx \theta$ and $\cos \theta \approx 1$ and ignoring higher order terms provides a linearized system and the discretized dynamics of the CartPole problem can be represented as for any t ,

$$\underbrace{\begin{bmatrix} y_{t+1} \\ \dot{y}_{t+1} \\ \theta_{t+1} \\ \dot{\theta}_{t+1} \end{bmatrix}}_{x_{t+1}} = \underbrace{\begin{bmatrix} 1 & \tau & 0 & 0 \\ 0 & 1 & -\frac{mlg\tau}{\eta(m+M)} & 0 \\ 0 & 0 & 1 & \tau \\ 0 & 0 & \frac{g\tau}{\eta} & 1 \end{bmatrix}}_A \underbrace{\begin{bmatrix} y_t \\ \dot{y}_t \\ \theta_t \\ \dot{\theta}_t \end{bmatrix}}_{x_t} + \underbrace{\begin{bmatrix} 0 \\ \frac{(m+M)\eta + ml}{(m+M)^2\eta} \tau \\ 0 \\ -\frac{\tau}{(m+M)\eta} \end{bmatrix}}_B u_t + f_t \left(y_t, \dot{y}_t, \theta_t, \dot{\theta}_t, u_t \right)$$

where $(y_t, \dot{y}_t, \theta_t, \dot{\theta}_t)^\top$ denotes the system state at time t ; τ denotes the time interval between state updates; $\eta := (4/3)l - ml/(m+M)$ and the function f_t measures the difference between the linearized system and the true system dynamics. Note that $f_t(\mathbf{0}) = 0$ for all time steps $t \geq 0$.

Policy setting. The pre-trained agents Stable-Baselines3 [13] of A2C [37], ARS [14], PPO [1] and TRPO [12] are selected as four candidate black-box policies. The CartPole environment is modified so that quadratic costs are considered rather than discrete rewards to match our control problem (3). The

Table 2: Hyper-parameters used in the real-world EV charging problem.

Parameter	Value
<i>Problem setting</i>	
Number of chargers n	5
Line limit γ (in kW)	6.6
Duration τ (in minute)	5
Reward coefficient ϕ_1	50
Reward coefficient ϕ_2	0.01
Reward coefficient ϕ_3	10
<i>Policy setting</i>	
Discount γ_{SAC}	0.9
Target smoothing coefficient τ_{SAC}	0.005
Temperature parameter α_{SAC}	0.2
Learning rate	$3 \cdot 10^{-4}$
Maximum number of steps	$10 \cdot 10^6$
Reply buffer size	$10 \cdot 10^6$
Number of hidden layers (all networks)	2
Number of hidden units per layer	256
Number of samples per minibatch	256
Nonlinearity	ReLU
<i>Training and testing data</i>	
Pre-COVID-19 (Training)	May, 2019 - Aug, 2019
Pre-COVID-19 (Testing)	Sep, 2019 - Dec, 2019
In-COVID-19	Feb, 2020 - May, 2020
Post-COVID-19	May, 2021 - Aug, 2021
CPU	Intel® i7-8850H

choices of Q and R in the costs and other parameters are provided in Table 1. Note that we vary the values of m and M in the LQR implementation to model the case of only having crude estimates of linear dynamics. The LQR outputs an action 0 if $-Kx_t + F' < 0$ and 1 otherwise. A shifted force $F' = 15$ is used to model inaccurate linear approximations and noise. The pre-trained RL policies output a binary decision $\{0, 1\}$ representing force directions. To use our adaptive policy in this setting, given a system state x_t at each time t , we implement the following:

$$u_t = \lambda_t (2\pi_{\text{RL}}(x_t)F - F) + (1 - \lambda_t) (2\pi_{\text{LQR}}(x_t)F - F)$$

where F is a fixed force magnitude defined in Table 1; π_{RL} denotes an RL policy; π_{LQR} denotes an LQR policy and λ_t is a confidence coefficient generated based on (6). Instead of fixing a step size α , we set an upper bound $\delta = 0.2$ on the learned step size λ' to avoid converging too fast to a pure model-based policy.

A.2 Real-world adaptive EV charging in tackling COVID-19

Problem setting. The second application considered is an EV charging problem modeled by real-world large-scale charging data [36]. The problem is formally described below.

Example 2 (Adaptive EV charging). *Consider the problem of managing a fleet of electric vehicle supply equipment (EVSE). Let n be the number of EV charging stations. Denote by $x_t \in \mathbb{R}_+^n$ the charging states of the n stations, i.e., $x_t^{(i)} > 0$ if an EV is charging at station- i and $x_t^{(i)}$ (kWh) energy*

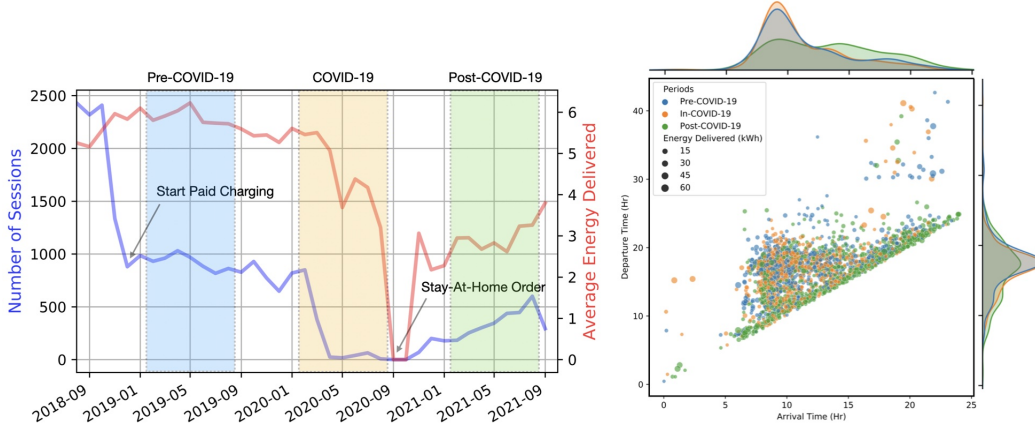


Figure 4: Illustration of the impact of COVID-19 on charging behaviors in terms of the total number of charging sessions and energy delivered (left) and distribution shifts (right).

needs to be delivered; otherwise $x_t^{(i)} = 0$. Let $u_t \in \mathbb{R}_+^n$ be the allocation of energy to the n stations. There is a line limit $\gamma > 0$ so that $\sum_{i=1}^n u_t^{(i)} \leq \gamma$ for any i and t . At each time t , new EVs may arrive and EVs being charged may depart from previously occupied stations. Each new EV j induces a charging session, which can be represented by $s_j := (a_j, d_j, e_j, i)$ where at time a_j , EV j arrives at station i , with a battery capacity $e_j > 0$, and depart at time d_j . Assuming lossless charging, the system dynamics is $x_{t+1} = x_t + u_t + f_t(x_t, u_t)$, $t \geq 0$ where the nonlinear residual functions ($f_t : t \geq 0$) represent uncertainty and constraint violations. Let τ be the time interval between state updates. Given fixed session information ($s_j : j > 0$), denote by the following sets containing the sessions that are assigned to a charger i and activated (deactivated) at time t :

$$\begin{aligned} \mathcal{A}_i &:= \left\{ (j, t) : a_j \leq t \leq a_j + \tau, s_j^{(4)} = i \right\}, \\ \mathcal{D}_i &:= \left\{ (j, t) : d_j \leq t \leq d_j + \tau, s_j^{(4)} = i \right\}. \end{aligned}$$

The charging uncertainty is summarized as for any $i = 1, \dots, n$,

$$f_t^{(i)}(x_t, u_t) := \begin{cases} s_j^{(3)} & \text{if } (j, t) \in \mathcal{A}_i & \text{(New sessions are active)} \\ -x_t^{(i)} - u_t^{(i)} & \text{if } (j, t) \in \mathcal{D}_i \text{ or } x_t^{(i)} + u_t^{(i)} < 0 & \text{(Sessions end/battery is full)} \\ \frac{\gamma}{\|u_t\|_1} u_t^{(i)} & \text{if } \sum_{i=1}^n u_t^{(i)} > \gamma & \text{(Line limit is exceeded)} \\ 0 & \text{otherwise} \end{cases}.$$

Note that the nonlinear residual functions ($f_t : t \geq 0$) in Example 2 may not satisfy $f_t(\mathbf{0}) = 0$ for all $t \geq 0$ in Assumption 1. Our experiments further validate that the adaptive policy works well in practice even if some of the model assumptions are violated. The goal of an EV charging controller is to maximize a system-level reward function including maximizing energy delivery, avoiding a penalty due to uncharged capacities and minimizing electricity costs. The reward function is

$$r(u_t, x_t) := \underbrace{\phi_1 \times \tau \|u_t\|_2}_{\text{Charging rewards}} - \underbrace{\phi_2 \times \|x_t\|_2}_{\text{Unfinished charging}} - \underbrace{\phi_3 \times p_t \|u_t\|_1}_{\text{Electricity cost}} - \underbrace{\phi_4 \times \sum_{i=1}^n \mathbf{1}((j, t) \in \mathcal{D}_i) \frac{x_t^{(i)}}{e_j}}_{\text{Penalty}}$$

with coefficients ϕ_1, ϕ_2, ϕ_3 and ϕ_4 shown in Table 2. The environment is wrapped as an OpenAI gym environment [35]. In our implementation, for convenience, the state x_t is in \mathbb{R}_+^{2n} with additional n coordinates representing remaining charging duration. The electricity prices ($p_t : t \geq 0$) are average

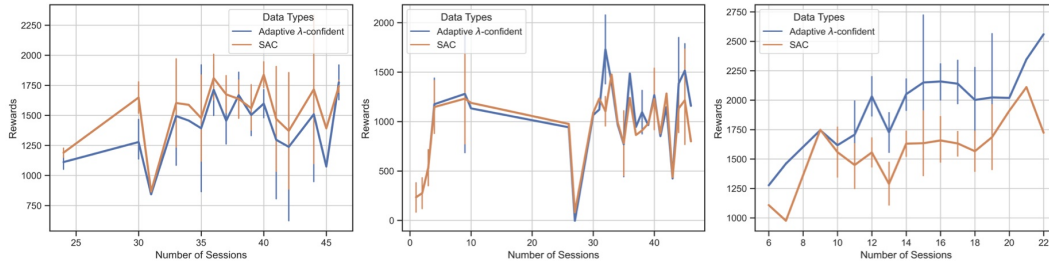


Figure 5: Bar-plots of rewards/number of sessions corresponding to testing the SAC policy and the adaptive policy on the EV charging environment based on sessions collected from three time periods.

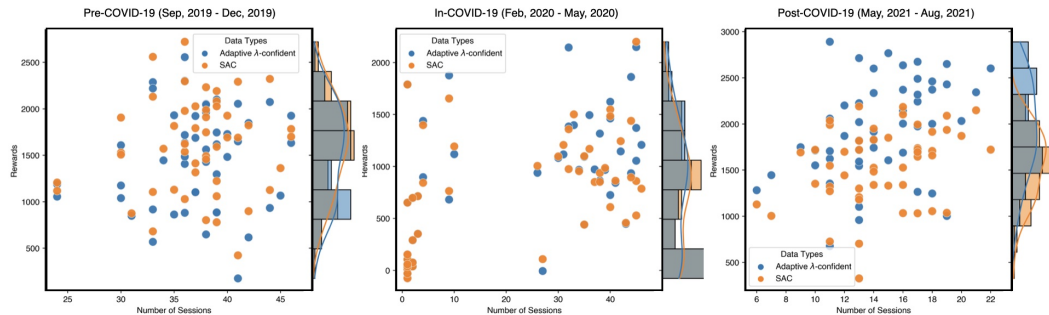


Figure 6: Supplementary results of Figure 3 with additional testing rewards for an in-COVID-19 period.

locational marginal prices (LMPs) on the CAISO (California Independent System Operator) day-ahead market in 2016.

Policy setting. We train an SAC [38] policy π_{SAC} for EV charging with 4-month data collected from a real-world charging garage [36] before the outbreak of COVID-19. The public charging infrastructure has 54 chargers and we use the charging history to set up our charging environment with 5 chargers. Knowledge of the linear parts in the nonlinear dynamics $x_{t+1} = x_t + u_t + f_t(x_t, u_t)$, $t \geq 0$ is assumed to be known, based on which an LQR controller π_{LQR} is constructed. Our adaptive policy presented in Algorithm 1 learns a confidence coefficient λ_t at each time step t to combine the two policies π_{SAC} and π_{LQR} .

Impact of COVID-19. We test the policies on different periods from 2019 to 2021. The impact of COVID-19 on the charging behavior is intuitive. As COVID-19 became an outbreak in early Feb, 2020 and later a pandemic in May, 2020, limited Stay at Home Order and curfew were issued, which significantly reduce the number of active users per day. Figure 4 illustrates the dramatic fall of the total number of monthly charging sessions and total monthly energy delivered between Feb, 2020 and Sep, 2020. Moreover, despite the recovery of the two factors since Jan, 2021, COVID-19 has a long-term impact on lifestyle behaviors. For example, the right sub-figure in Figure 4 shows that the arrival times of EVs (start times of sessions) are flattened in the post-COVID-19 period, compared to a more concentrated arrival peak before COVID-19. The significant shift of distributions highly deteriorates the performance of DNN-based model-free policies, e.g., SAC that are trained on normal charging data collected before COVID-19. In this work, we demonstrate that taking advantage of model-based information, the adaptive λ -confident policy (Algorithm 1) is able to correct the mistakes made by DNN-based model-free policies trained on biased data and achieve more robust charging performance.

Additional experimental results. We provide supplementary experimental results. Besides comparing the periods of pre-COVID-19 and post-COVID-19, we include the testing rewards for an in-COVID-19 period in Figure 6, together with the corresponding bar-plots in Figure 5. In addition, the average total rewards for the SAC policy and the adaptive policy are summarized in Table 3.

Table 3: Average total rewards for the SAC policy and the adaptive λ -confident policy (Algorithm 1).

<i>Policy</i>	Pre-COVID-19	In-COVID-19	Post-COVID-19
SAC [38]	1601.914	765.664	1540.315
Adaptive	1489.338	839.651	1951.192

B Notation and Supplementary Definitions

B.1 Summary of notation

A summary of notation is provided in Table 4.

Symbol	Definition
<i>System Model</i>	
A, B, Q, R	Linear system parameters
P	Solution of the DARE (4)
H	$R + B^\top PB$
K	$H^{-1}B^\top PA$
F	$A - BK$
σ	$Q, R \succeq \sigma I$
κ	$\max\{2, \ A\ , \ B\ \}$
C_F and ρ	$\ F^t\ \leq C_F \rho^t$
$f_t : \mathbb{R}^n \times \mathbb{R}^m \rightarrow \mathbb{R}^n$	Nonlinear residual functions
C_ℓ	Lipschitz constant of f_t
$\hat{\pi}$	Black-box (model-free) policy
$\bar{\pi}$	Model-based policy (LQR)
ε	Consistency error of a black-box policy
<i>Main Results</i>	
$C_a^{\text{sys}}, C_b^{\text{sys}}, C_c^{\text{sys}}$	Constants defined in Section B.2
γ	$\rho + C_F C_\ell (1 + \ K\)$
μ	$C_F (\varepsilon (C_\ell + \ B\) + C_a^{\text{sys}} C_\ell)$
ALG	Algorithm cost
OPT	Optimal cost
$\text{CR}(\varepsilon)$	$2\kappa \left(\frac{C_F \ F\ }{1-\rho}\right)^2 / \sigma$
λ	$\lim_{t \rightarrow \infty} \lambda_t$
t_0	The smallest time index when $\lambda_t = 0$ or $x_t = \mathbf{0}$

Table 4: Symbols used in this work.

B.2 Constants in Theorem 2 and 3

Let $H := R + B^\top PB$. With $\sigma > 0$ defined in Assumption 2, the parameters $C_a^{\text{sys}}, C_b^{\text{sys}}, C_c^{\text{sys}} > 0$ in the statements of Theorem 2 and 3 (Section 4) are the following constants that only depend on the known system parameters in (3):

$$\begin{aligned}
C_a^{\text{sys}} &:= 1 / \left(2C_F \|R + B^\top PB\|^{-1} \left(\|PF\| + (1 + \|K\|) (\|PB\| + \|P\|) \right. \right. \\
&\quad \left. \left. + \frac{C_b^{\text{sys}}}{2} \|B + I\| (1 + \|F\| + \|K\|) \right) \right), \\
C_b^{\text{sys}} &:= \frac{2C_F^2 \|P\| (\rho + \bar{C}) (\rho + (1 + \|K\|))}{1 - (\rho + \bar{C})^2} \sqrt{\frac{\|Q + K^\top RK\|}{\sigma}}, \\
C_c^{\text{sys}} &:= \|H\| / (4 \|PB\| + 2 \|P\| + C_\nabla (\|B\| + 1) \|B\|).
\end{aligned} \tag{7}$$

B.3 Approximations in online learning steps Section 5.1

The following approximations of $\eta(\hat{f}; s, t)$ and $\eta(f^*; s, t)$ in (5) are used to derive the expression of λ' in (6) for learning the confidence coefficients online:

$$\eta(\hat{f}; s, t) \approx \sum_{\tau=s}^{\infty} \left(F^\top \right)^{\tau-s} P \hat{f}_\tau = - \left(H^{-1} B^\top \right)^\dagger (\hat{u}_s + K x_s), \tag{8}$$

$$\eta(f^*; s, t) = \sum_{\tau=s}^t \left(F^\top \right)^{\tau-s} P f_\tau^* \approx \sum_{\tau=s}^t \left(F^\top \right)^{\tau-s} P (x_{\tau+1} - A x_\tau - B u_\tau). \tag{9}$$

C Useful Lemmas

The following lemma generalizes the results in [39].

Lemma 1 (Generalized cost characterization lemma). *Consider a linear quadratic control problem below where $Q, R \succ 0$ and the pair of matrices (A, B) is stabilizable:*

$$\min_{(u_t: t \geq 0)} \sum_{t=0}^{\infty} (x_t^\top Q x_t + u_t^\top R u_t), \text{ subject to } x_{t+1} = A x_t + B u_t + v_t \text{ for any } t \geq 0.$$

If at each time $t \geq 0$, $u_t = -K x_t - H^{-1} B^\top W_t + \eta_t$ where $\eta_t \in \mathbb{R}^m$, then the induced cost is

$$\begin{aligned}
&x_0^\top P x_0 + 2x_0^\top F^\top V_0 + \sum_{t=0}^{\infty} \eta_t^\top H \eta_t + \sum_{t=0}^{\infty} \left(v_t^\top P v_t + 2v_t^\top F^\top V_{t+1} \right) \\
&+ \sum_{t=0}^{\infty} \left(W_t^\top B H^{-1} B^\top (W_t - 2V_t) + 2\eta_t^\top B^\top (V_t - W_t) \right) + O(1)
\end{aligned}$$

where P is the unique solution of the DARE in (4), $H := R + B^\top PB$, $F := A - B(R + B^\top PB)^{-1} B^\top PA = A - BK$, $W_t := \sum_{\tau=t}^{\infty} (F^\top)^\tau P w_{t+\tau}$ and $V_t := \sum_{\tau=t}^{\infty} (F^\top)^\tau P v_{t+\tau}$.

Proof. Denote by $\text{COST}_t(x_t; \eta, w)$ the terminal cost at time t given a state x_t with fixed action perturbations $\eta := (\eta_t : t \geq 0)$ and state perturbations $w := (w_t : t \geq 0)$. We assume $\text{COST}_t(x_t; \eta, w) := x_t^\top P x_t + p_t^\top x_t + q_t$. Similar to the proof of Lemma 13 in [39], using the backward induction, the cost can be rewritten as

$$\begin{aligned}
\text{COST}_t(x_t; \eta, w) &= \text{COST}_{t+1}(x_{t+1}; \eta, w) + x_t^\top Q x_t + u_t^\top R u_t \\
&= x_t^\top Q x_t + u_t^\top R u_t + (A x_t + B u_t + v_t)^\top P (A x_t + B u_t + v_t) \\
&\quad + p_{t+1}^\top (A x_t + B u_t + v_t) + q_{t+1} \\
&= x_t^\top Q x_t + (A x_t + v_t)^\top P (A x_t + v_t) + (A x_t + v_t)^\top p_{t+1} + q_{t+1} \\
&\quad + \underbrace{u_t^\top (R + B^\top PB) u_t}_{(a)} + \underbrace{2u_t^\top B^\top (P A x_t + P v_t + p_{t+1}/2)}_{(b)}.
\end{aligned}$$

Denote by $H := R + B^\top PB$. Noting that $u_t = -Kx_t + G_t + \eta_t$ where we denote

$$G_t := H^{-1}B^\top W_t, \quad W_t := \sum_{\tau=t}^{\infty} \left(F^\top\right)^\tau P w_{t+\tau} \text{ and } V_t := \sum_{\tau=t}^{\infty} \left(F^\top\right)^\tau P v_{t+\tau},$$

it follows that

$$\begin{aligned} (a) &= (Kx_t + G_t - \eta_t)^\top H (Kx_t + G_t - \eta_t) - 2(Kx_t)^\top H (G_t - \eta_t) \\ &\quad + (G_t - \eta_t)^\top (R + B^\top PB)(G_t - \eta_t) \\ (b) &= -2(Kx_t)^\top H (Kx_t) - 2x_t^\top K^\top B^\top P v_t - x_t^\top K^\top B^\top p_{t+1} - 2(Kx_t)^\top H (G_t - \eta_t) \\ &\quad - 2(G_t - \eta_t)^\top B^\top (P v_t + p_{t+1}/2), \end{aligned}$$

implying

$$\begin{aligned} \text{COST}_t(x_t; \eta, w) &= x_t^\top (Q + A^\top PA - K^\top HK)x_t + x_t^\top F^\top (2P v_t + p_{t+1}) \\ &\quad + (G_t - \eta_t)^\top H (G_t - \eta_t) - 2(G_t - \eta_t)^\top B^\top (P v_t + p_{t+1}/2) \\ &\quad + v_t^\top P v_t + v_t^\top p_{t+1} + q_{t+1}. \end{aligned}$$

According to the DARE in (4), since $K^\top HK = A^\top PB(R + B^\top PB)^{-1}B^\top PA$, we get

$$\begin{aligned} \text{COST}_t(x_t; \eta, w) &= x_t^\top P x_t + x_t^\top F^\top (2P v_t + p_{t+1}) + (G_t - \eta_t)^\top H (G_t - \eta_t) \\ &\quad - 2(G_t - \eta_t)^\top B^\top (P v_t + p_{t+1}/2) + v_t^\top P v_t + v_t^\top p_{t+1} + q_{t+1}, \end{aligned}$$

which implies

$$p_t = 2F^\top (P v_t + p_{t+1}) = 2 \sum_{\tau=t}^{\infty} \left(F^\top\right)^{\tau+1} P v_{t+\tau} = 2F^\top V_t, \quad (10)$$

$$\begin{aligned} q_t &= q_{t+1} + v_t^\top P v_t + 2v_t^\top F^\top V_{t+1} + (G_t - \eta_t)^\top H (G_t - \eta_t) \\ &\quad - 2(G_t - \eta_t)^\top B^\top (P v_t + p_{t+1}/2) \\ &= q_{t+1} + v_t^\top P v_t + 2v_t^\top F^\top V_{t+1} + (G_t - \eta_t)^\top H (G_t - \eta_t) \\ &\quad - 2G_t^\top B^\top V_t + 2\eta_t^\top B^\top V_t \\ &= q_{t+1} + v_t^\top P v_t + 2v_t^\top F^\top V_{t+1} + G_t^\top B^\top (W_t - 2V_t) + 2\eta_t^\top B^\top (V_t - W_t) + \eta_t^\top H \eta_t. \quad (11) \end{aligned}$$

Therefore, (10) and (11) together imply the following general cost characterization:

$$\begin{aligned} \text{COST}_t(x_t; \eta, w) &= x_0^\top P x_0 + x_0^\top p_0 + q_0 \\ &= x_0^\top P x_0 + 2x_0^\top F^\top V_0 + \sum_{t=0}^{\infty} \eta_t^\top H \eta_t + \sum_{t=0}^{\infty} \left(v_t^\top P v_t + 2v_t^\top F^\top V_{t+1}\right) \\ &\quad + \sum_{t=0}^{\infty} \left(G_t^\top B^\top (W_t - 2V_t) + 2\eta_t^\top B^\top (V_t - W_t)\right). \end{aligned}$$

Rearranging the terms above completes the proof. \square

To deal with the nonlinear dynamics in (1), we consider an auxiliary linear system, with a fixed perturbation $w_t = f_t(x_t^*, u_t^*)$ for all $t \geq 0$ where each x_t^* denotes an optimal state and u_t^* an optimal action, generated by an optimal policy π^* . We define a sequence of linear policies $(\pi'_t : t \geq 0)$ where $\pi'_t : \mathbb{R}^n \rightarrow \mathbb{R}^m$ generates an action

$$u'_t = \pi'_t(x_t) := -(R + B^\top PB)^{-1}B^\top \left(P A x_t + \sum_{\tau=t}^{\infty} \left(F^\top\right)^{\tau-t} P f_\tau(x_\tau^*, u_\tau^*) \right), \quad (12)$$

which is an optimal policy for the auxiliary linear system. Utilizing Lemma 1, the gap between the optimal cost and algorithm cost for the system in (3) can be characterized below.

Lemma 2. For any $\eta_t \in \mathbb{R}^m$, if at each time $t \geq 0$, a policy $\pi : \mathbb{R}^n \rightarrow \mathbb{R}^m$ takes an action $u_t = \pi(x_t) = \pi'_t(x_t) + \eta_t$, then the gap between the optimal cost OPT of the nonlinear system (3) and the algorithm cost ALG induced by selecting control actions ($u_t : t \geq 0$) equals to

$$\begin{aligned}
\text{ALG} - \text{OPT} &\leq \sum_{t=0}^{\infty} \eta_t^\top H \eta_t + O(1) \\
&+ 2 \sum_{t=0}^{\infty} \eta_t^\top B^\top \left(\sum_{\tau=t}^{\infty} (F^\top)^\tau P (f_{t+\tau} - f_{t+\tau}^*) \right) \\
&+ \sum_{t=0}^{\infty} \left(f_t^\top P f_t - (f_t^*)^\top P f_t^* \right) + 2x_0^\top \left(\sum_{t=0}^{\infty} (F^\top)^{t+1} P (f_t - f_t^*) \right) \\
&+ 2 \sum_{t=0}^{\infty} \left(f_t^\top \sum_{\tau=0}^{\infty} (F^\top)^{\tau+1} P f_{t+\tau+1} - (f_t^*)^\top \sum_{\tau=0}^{\infty} (F^\top)^{\tau+1} P (f_{t+\tau+1}^*) \right) \\
&+ 2 \sum_{t=0}^{\infty} \left(\sum_{\tau=t}^{\infty} (F^\top)^\tau P f_{t+\tau}^* \right) B H^{-1} B^\top \left(\sum_{\tau=t}^{\infty} (F^\top)^\tau P (f_{t+\tau}^* - f_{t+\tau}) \right) \quad (13)
\end{aligned}$$

where $H := R + B^\top P B$ and $F := A - BK$. For any $t \geq 0$, we write $f_t := f_t(x_t, u_t)$ and $f_t^* := f_t(x_t^*, u_t^*)$ where $(x_t : t \geq 0)$ denotes a trajectory of states generated by the policy π with actions ($u_t^* : t \geq 0$) and $(x_t^* : t \geq 0)$ denotes an optimal trajectory of states generated by optimal actions ($u_t^* : t \geq 0$).

Proof. Note that with optimal trajectories of states and actions fixed, the optimal controller π^* induces the same cost OPT for both the nonlinear system in (3) and the auxiliary linear system. Moreover, the linear controller defined in (12) induces a cost OPT' that is smaller than OPT when running both in the auxiliary linear system since the constructed linear policy is optimal. Therefore, according to Lemma 1, $\text{ALG} - \text{OPT} \leq \text{ALG} - \text{OPT}'$ and applying Lemma 1 with $v_t = f_t(x_t, u_t)$ and $w_t = f_t(x_t^*, u_t^*)$ for all $t \geq 0$, (13) is obtained. \square

D Proof of Theorem 1

Proof. Fix an arbitrary controller K_1 with a closed-loop system matrix $F_1 := A - BK_1 \neq 0$. We first consider the case when F_1 is not a diagonal matrix, i.e., $A - BK_1$ has at least one non-zero off-diagonal entry. Consider the following closed-loop system matrix for the second controller K_2 :

$$F_2 := \begin{pmatrix} \beta & & \cdots & \\ & \beta & & \mathbf{0} \\ & & \ddots & \\ -\frac{1-\lambda}{\lambda} \bar{L} & & & \beta \\ & & & & \beta \end{pmatrix} + S(F_1) \quad (14)$$

where $0 < \beta < 1$ is a value of the diagonal entry; \bar{L} is the lower triangular part of the closed-loop system matrix F_1 . The matrix $S(F_1)$ is a singleton matrix that depends on F_1 , whose only non-zero entry $S_{i+k,i}$ corresponding to the first non-zero off-diagonal entry $(i, i+k)$ in the upper triangular part of F_1 searched according to the order $i = 1, \dots, n$ and $k = 1, \dots, n$ with i increases first and then k . Such a non-zero entry always exists because in this case F_1 is not a diagonal matrix. If the non-zero off-diagonal entry appears to be in the lower triangular part, we can simply transpose F_2 so without loss of generality we assume it is in the upper triangular part of F_1 . Since F_1 is a lower triangular matrix, all of its eigenvalues equal to $0 < \beta < 1$, implying that the linear controller K_2 is stabilizing. Then,

based on the construction of F_1 in (14), the linearly combined controller $K := \lambda K_2 + (1 - \lambda)K_1$ has a closed-loop system matrix F which is upper-triangular, whose determinant satisfies

$$\begin{aligned} \det(F) &= \det(\lambda F_2 + (1 - \lambda)F_1) \\ &= (-1)^{2i+k} \det(F') \end{aligned} \quad (15)$$

$$= (-1)^{2i+k} \times (-1)^{k+1} (1 - \lambda) \lambda^{n-1} S_{i+k,i}(F_1)_{i,i+k} \beta^{n-2} \quad (16)$$

$$= -S_{i+k,i} (1 - \lambda) \lambda^{n-1} \beta^{n-2} \quad (17)$$

where the term $(-1)^{2i+k}$ in (15) comes from the computation of the determinant of F and F' is a sub-matrix of F by eliminating the $i + k$ -th row and i -th column. The term $(-1)^{k+1}$ in (16) appears because F' is a permutation of an upper triangular matrix with $n - 2$ diagonal entries being β 's and one remaining entry being $(F_1)_{i,i+k}$ since the entries $S_{j,j+k}$ are zeros all $j < i$; otherwise another non-zero entry $S_{i+k,i}$ would be chosen according to our search order.

Continuing from (17), since $S_{i+k,i}$ can be selected arbitrarily, setting $S_{i+k,i} = \frac{-2^n \beta (\lambda \beta)^{-n+1}}{1-\lambda}$ gives

$$2^n \leq \det(F) \leq |\rho(F)|^n,$$

implying that the spectral radius $\rho(F) \geq 2$. Therefore $K = \lambda K_2 + (1 - \lambda)K_1$ is an unstable controller. It remains to prove the theorem in the case when F_1 is a diagonal matrix. In the following lemma, we consider the case when $n = 2$, and extend it to the general case.

Lemma 3. *For any $\lambda \in (0, 1)$ and any diagonal matrix $F_1 \in \mathbb{R}^{2 \times 2}$ with a spectral radius $\rho(F_1) < 1$ $F_1 \neq \gamma I$ for any $\gamma \in \mathbb{R}$, there exists a matrix $F_2 \in \mathbb{R}^{2 \times 2}$ such that $\rho(F_2) < 1$ and $\rho(\lambda F_1 + (1 - \lambda)F_2) > 1$.*

Proof of Lemma 3. Suppose $n = 2$ and

$$F_1 = \begin{bmatrix} a & 0 \\ 0 & b \end{bmatrix}$$

is a diagonal matrix and without loss of generality assume that $a > 0$ and $a > b$. Let

$$F_2 = \frac{4}{\lambda(1 - \lambda)(a - b)} \begin{bmatrix} 1 & 1 \\ -1 & -1 \end{bmatrix}. \quad (18)$$

Notice that $\rho(F_2) = 0 < 1$ satisfies the constraint. Then

$$\begin{aligned} \rho(\lambda F_1 + (1 - \lambda)F_2) &= \rho(\lambda b I + \lambda \text{Diag}(a - b, 0) + (1 - \lambda)F_2) \\ &= \lambda b + \rho(\lambda \text{Diag}(a - b, 0) + (1 - \lambda)F_2) \end{aligned} \quad (19)$$

where we have used the assumption that $a > 0$ and $a > b$ to derive the equality in (19) and the notion $\text{Diag}(a - b, 0)$ denotes a diagonal matrix whose diagonal entries are $a - b$ and 0 respectively. The eigenvalues of $\lambda \text{Diag}(a - b, 0) + (1 - \lambda)F_2$ are

$$\frac{\lambda(a - b) \pm \sqrt{(\lambda(a - b) + \frac{8}{\lambda(a - b)})^2 - 4(\frac{4}{\lambda(a - b)})^2}}{2} = \frac{\lambda(a - b) \pm \sqrt{(\lambda(a - b))^2 + 16}}{2}.$$

Since $a - b > 0$, the spectral radius of $\lambda F_1 + (1 - \lambda)F_2$ satisfies

$$\rho(\lambda F_1 + (1 - \lambda)F_2) = \lambda b + \frac{\lambda(a - b) + \sqrt{(\lambda(a - b))^2 + 16}}{2} > -1 + \frac{\sqrt{16}}{2} = 1. \quad \square$$

Applying Lemma 3, when F_1 is an $n \times n$ matrix with $n > 2$, we can always create an $n \times n$ matrix F_2 whose first two columns and rows form a sub-matrix that is the same as (18) and the remaining entries are zeros. Therefore the spectral radius of the convex combination $\lambda F_1 + (1 - \lambda)F_2$ is greater than one. This completes the proof. \square

E Stability Analysis

E.1 Proof outline

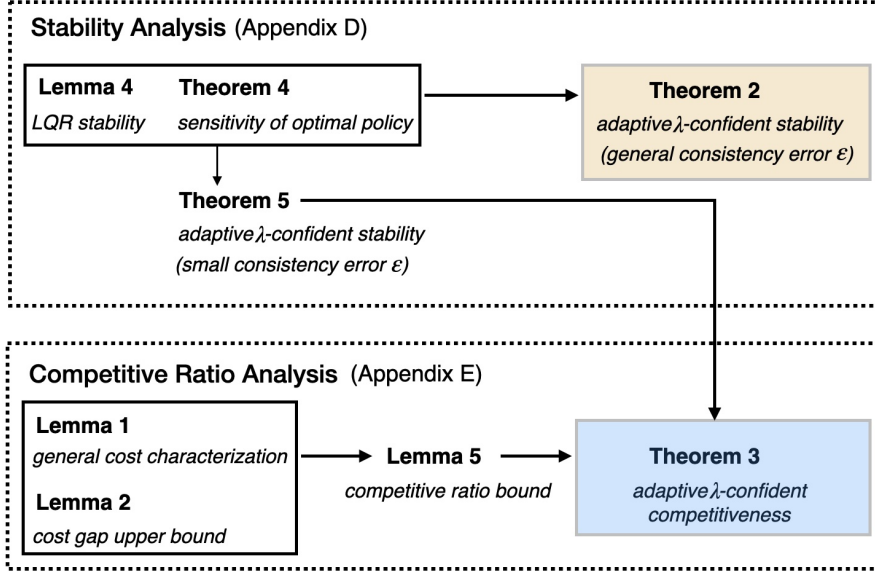


Figure 7: Outline of proofs of Theorem 2 and 3 with a stability analysis presented in Appendix E and a competitive ratio analysis presented in Appendix F. Arrows denote implications.

In the sequel, we present the proofs of Theorem 2 and 3. An outline of the proof structure is provided in Figure 7. The proof of our main results contains two parts – the *stability analysis* and *competitive ratio analysis*. First, we prove that Algorithm 1 guarantees a stabilizing policy, regardless of the prediction error ε (Theorem 2). Second, in our competitive ratio analysis, we provide a competitive ratio bound in terms of ε and λ . We show in Lemma 5 that the competitive ratio bound is bounded if the adaptive policy is exponentially stabilizing and has a decay ratio that scales up with C_ℓ , which holds assuming the prediction error ε for a black-box model-free policy is small enough, as shown in Theorem 5. Theorem 5 is proven based on a sensitivity analysis of an optimal policy π^* in Theorem 4.

We first analyze the model-based policy $\hat{\pi}(x) = -Kx$ where $K := (R + B^\top PB)^{-1}B^\top PA$ and P is a unique solution of the Riccati equation in (4).

Lemma 4. *Suppose the Lipschitz constant C_ℓ , K and the closed-loop matrix $F := A - BK$ satisfy $\rho + C_F C_\ell (1 + \|K\|) < 1$ where $\|F^t\| \leq C_F \rho^t$ for any $t \geq 0$. Then the model-based policy $\hat{\pi}(x) = -Kx$ exponentially stabilizes the system such that $\|x_t\| \leq C_F (\rho + C_F \bar{C})^t \|x_0\|$ for any $t \geq 0$.*

Proof. Let $u_t = \hat{\pi}(x_t) = -Kx_t$ for all $t \geq 0$ and let $F := A - BK$. It follows that

$$x_{t+1} = Ax_t + Bu_t + f_t(x_t, u_t) = (A - BK)x_t + f_t(x_t, -Kx_t) = Fx_t + f_t(x_t, -Kx_t). \quad (20)$$

Rewriting (20) recursively, for any $t \geq 0$,

$$x_t = F^t x_0 + \sum_{\tau=0}^{t-1} F^{t-1-\tau} f_\tau(x_\tau, -Kx_\tau). \quad (21)$$

Since $(f_t : t \geq 0)$ are Lipschitz continuous with a constant C_ℓ (Assumption 1), we have

$$\begin{aligned}
\|x_t\| &\leq \|F^t x_0\| + \left\| \sum_{\tau=0}^{t-1} F^{t-1-\tau} f_\tau(x_\tau, -Kx_\tau) \right\| \\
&\leq \|F^t x_0\| + \sum_{\tau=0}^{t-1} \|F^{t-1-\tau} f_\tau(x_\tau, -Kx_\tau)\| \\
&\leq C_F \rho^t \underbrace{\left(\|x_0\| + C_\ell(1 + \|K\|) \sum_{\tau=0}^{t-1} \rho^{-1-\tau} \|x_\tau\| \right)}_{:=S_t}
\end{aligned} \tag{22}$$

where $C_F > 1$ is a constant such that $\|F^t\| \leq C_F \rho^t$ for any $t \geq 0$. Denote by $\bar{C} := C_\ell(1 + \|K\|)$. Then, using (22),

$$S_t = S_{t-1} + \bar{C} \rho^{-t} \|x_{t-1}\| \leq S_{t-1} + \frac{C_F \bar{C}}{\rho} S_{t-1} = \left(1 + \frac{C_F \bar{C}}{\rho}\right) S_{t-1}.$$

Therefore, noting that $S_1 = (1 + \bar{C}/\rho) \|x_0\|$, recursively we obtain

$$S_t \leq \left(1 + \frac{C_F \bar{C}}{\rho}\right)^{t-1} \left(1 + \frac{\bar{C}}{\rho}\right) \|x_0\|,$$

which implies

$$\begin{aligned}
\|x_t\| &\leq C_F \rho^t S_t \leq C_F \rho^t \left(1 + \frac{C_F \bar{C}}{\rho}\right)^{t-1} \left(1 + \frac{\bar{C}}{\rho}\right) \|x_0\| \\
&= C_F (\rho + C_F \bar{C})^{t-1} (\rho + \bar{C}) \|x_0\| \\
&\leq C_F (\rho + C_F \bar{C})^t \|x_0\|.
\end{aligned}$$

□

Next, based on Lemma 4, we consider the stability of the convex-combined policy $\pi = \lambda \hat{\pi} + (1-\lambda) \bar{\pi}$ where $\bar{\pi}$ is a model-free policy satisfying the ε -consistency in Definition 1 and $\hat{\pi}$ is a model-based policy.

Theorem 4. *Let π^* be an optimal policy and $\bar{\pi}(x) = -Kx$ be a linear model-based policy. It follows that for any $t \geq 0$, $\|\pi_t^*(x) - \bar{\pi}(x)\| \leq C_a^{\text{sys}} C_\ell \|x\|$ for some constant $C_a^{\text{sys}} > 0$ where C_ℓ is the Lipschitz constant defined in Assumption 1 and*

$$\begin{aligned}
C_a^{\text{sys}} &:= 2\|R + B^\top PB\|^{-1} \left(\|PF\| + (1 + \|K\|) (\|PB\| + \|P\|) \right. \\
&\quad \left. + \frac{C_b^{\text{sys}}}{2} \|B + I\| (1 + \|F\| + \|K\|) \right), \\
C_b^{\text{sys}} &:= \frac{2C_F^2 \|P\| (\rho + \bar{C}) (\rho + (1 + \|K\|))}{1 - (\rho + \bar{C})^2} \sqrt{\frac{\|Q + K^\top RK\|}{\sigma}}.
\end{aligned}$$

Proof. We use $\pi_t^*(x) = -Kx + h_t(x)$ to characterize an optimal policy at each time $t \geq 0$. Consider the following Bellman optimality equation:

$$V_t(x) = \min_u \{x^\top Qx + u_t^\top Ru_t + V_{t+1}(Ax + Bu + f_t(x, u))\} \tag{23}$$

where $V_t : \mathbb{R}^n \rightarrow \mathbb{R}_+$ denotes the optimal value function. Using lemma 4,

$$\begin{aligned}
V_t(x) &\leq x^\top (Q + K^\top RK)x + V_{t+1}(F^\top x + f_t(x, u)) \\
&\leq V_\infty(0) + \|Q + K^\top RK\| \sum_{t=0}^{\infty} C_F^2 (\rho + C_F \bar{C})^{2t} \|x\|^2 \\
&= V_\infty(0) + \frac{C_F^2 \|Q + K^\top RK\|}{1 - (\rho + C_F \bar{C})^2} \|x\|^2.
\end{aligned} \tag{24}$$

Let $x_t^{(\tau)}$ be the $(t + \tau)$ -th state when applying optimal control with $x_t = x$ and write $u_t^{(\tau)} = \pi_{t+\tau}^*(x_t^{(\tau)})$ for all $t \geq 0$. Rearranging the terms in (24), it follows that

$$\begin{aligned}
\frac{C_F^2 \|Q + K^\top RK\|}{1 - (\rho + C_F \bar{C})^2} \|x\|^2 &\geq V_t(x) - V_\infty(0) = \sum_{\tau=t}^{\infty} \left(x_t^{(\tau-t)}\right)^\top Q x_t^{(\tau-t)} + \left(u_t^{(\tau-t)}\right)^\top R u_t^{(\tau-t)} \\
&\geq \lambda_{\min}(Q) \sum_{\tau=0}^{\infty} \|x_t^{(\tau)}\|^2 + \lambda_{\min}(R) \sum_{\tau=0}^{\infty} \|u_t^{(\tau)}\|^2.
\end{aligned}$$

Write $V_t(x) = x^\top P x + g_t(x)$ with P denoting the solution of the Riccati equation in (4). Then

$$\begin{aligned}
&x^\top P x + g_t(x) \\
&= \min_u \left[x^\top Q x + u^\top R u + (Ax + Bu)^\top P (Ax + Bu) \right. \\
&\quad \left. + 2(Ax + Bu)^\top P f_t(x, u) + f_t(x, u)^\top P f_t(x, u) + g_{t+1}(Ax + Bu + f_t(x, u)) \right] \\
&= \min_u \left[x^\top (Q + A^\top P A)x + u^\top (R + B^\top P B)u + 2u^\top B^\top P A x + 2(Ax + Bu)^\top P f_t(x, u) \right. \\
&\quad \left. + f_t(x, u)^\top P f_t(x, u) + g_{t+1}(Ax + Bu + f_t(x, u)) \right] \\
&= \min_u \left[x^\top (Q + A^\top P A - A^\top P B (R + B^\top P B)^{-1} B^\top P A)x \right. \\
&\quad \left. + (u + (R + B^\top P B)^{-1} B^\top P A x)^\top (R + B^\top P B) (u + (R + B^\top P B)^{-1} B^\top P A x) \right. \\
&\quad \left. + 2(Ax + Bu)^\top P f_t(x, u) + f_t(x, u)^\top P f_t(x, u) + g_{t+1}(Ax + Bu + f_t(x, u)) \right].
\end{aligned}$$

Since P is the solution of the DARE in (4), letting $u = -Kx + v$ and $F := A - BK$,

$$\begin{aligned}
g_t(x) &= \min_v \left[v^\top (R + B^\top P B)v + 2x^\top F^\top P f_t(x, -Kx + v) + 2v^\top B^\top P f_t(x, -Kx + v) \right. \\
&\quad \left. + f_t(x, -Kx + v)^\top P f_t(x, -Kx + v) + g_{t+1}(Fx + Bv + f_t(x, -Kx + v)) \right].
\end{aligned}$$

Denoting by v_t^* an optimal solution,

$$\begin{aligned}
g_t(x) &= (v_t^*)^\top (R + B^\top P B)v_t^* + 2x^\top F^\top P f_t(x, -Kx + v_t^*) + 2(v_t^*)^\top B^\top P f_t(x, -Kx + v_t^*) \\
&\quad + f_t(x, -Kx + v_t^*)^\top P f_t(x, -Kx + v_t^*) + g_{t+1}(Fx + Bv_t^* + f_t(x, -Kx + v_t^*)).
\end{aligned}$$

Denote by ∇g_t the Jacobian of g_t . We obtain

$$\begin{aligned}
\nabla g_t(x) &= 2(R + B^\top P B)v_t^* \nabla v_t^* \\
&\quad + 2F^\top P f_t(x, -Kx + v_t^*) \\
&\quad + 2x^\top F^\top P \nabla f_t(x, -Kx + v_t^*) [I, -K + \nabla v_t^*] \\
&\quad + 2\nabla (v_t^*)^\top B^\top P f_t(x, -Kx + v_t^*) \\
&\quad + 2(v_t^*)^\top B^\top P \nabla f_t(x, -Kx + v_t^*) [I, -K + \nabla v_t^*] \\
&\quad + 2P f_t(x, -Kx + v_t^*) \nabla f_t(x, -Kx + v_t^*) [I, -K + \nabla v_t^*] \\
&\quad + \nabla g_{t+1}(Fx + Bv_t^* + f_t(x, -Kx + v_t^*)) (F + B\nabla v_t^* + \nabla f_t(x, -Kx + v_t^*) [I, -K + \nabla v_t^*])
\end{aligned}$$

Noting that v_t^* is a minimizer, the Jacobian of g_t with respect to v takes zero at $v = v_t^*$:

$$\begin{aligned} & 2(R + B^\top PB)v + 2x^\top F^\top P \nabla f_t(x, -Kx + v)[0, I] + 2B^\top P f_t(x, -Kx + v) \\ & + 2v^\top B^\top P \nabla f_t(x, -Kx + v)[0, I] + 2P f_t(x, -Kx + v) \nabla f_t(x, -Kx + v)[0, I] \\ & + (B + \nabla f_t(x, -Kx + v)[0, I])^\top \nabla g_{t+1}(Fx + Bv + f_t(x, -Kx + v))|_{v=v_t^*} = 0 \end{aligned} \quad (25)$$

Substituting above into the Jacobian of g_t , we get

$$\begin{aligned} \nabla g_t(x) &= 2F^\top P f_t(x, -Kx + v_t^*) \\ &+ 2x^\top F^\top P \nabla f_t(x, -Kx + v_t^*)[I, -K] \\ &+ 2(v_t^*)^\top B^\top P \nabla f_t(x, -Kx + v_t^*)[I, -K] \\ &+ 2P f_t(x, -Kx + v_t^*) \nabla f_t(x, -Kx + v_t^*)[I, -K] \\ &+ \nabla g_{t+1}(Fx + Bv_t^* + f_t(x, -Kx + v_t^*))(F + \nabla f_t(x, -Kx + v_t^*)[I, -K]) \\ &= 2F^\top P f_t(x, -Kx + v_t^*) + 2(\nabla f_t(x, -Kx + v_t^*)[I, K])^\top P x \\ &+ (F + \nabla f_t(x, -Kx + v_t^*)[I, -K])^\top \nabla g_{t+1}(x_t^{(1)}), \end{aligned}$$

which implies that

$$\begin{aligned} \nabla g_t(x) &= \prod_{\tau=t}^{\infty} (F + \nabla f_\tau(x_t^{(\tau-t)}, u_t^{(\tau-t)})[I, -K])^\top g_\infty(0) \\ &+ \sum_{\tau=t}^{\infty} \prod_{k=t}^{\tau} (F + \nabla f_k(x_t^{(k-t)}, u_t^{(k-t)})[I, -K])^\top 2F^\top P f_\tau(x_t^{(\tau-t)}, u_t^{(\tau-t)}) \\ &+ \sum_{\tau=t}^{\infty} \prod_{k=t}^{\tau} (F + \nabla f_k(x_t^{(k-t)}, u_t^{(k-t)})[I, -K])^\top 2(\nabla f_\tau(x_\tau^{(\tau-t)}, u_\tau^{(\tau-t)})[I, -K])^\top P_{\tau+1}^*. \end{aligned} \quad (26)$$

Note that for any sequence of pairs $((x_t^{(\tau)}, u_t^{(\tau)}) : \tau \geq 0)$,

$$\begin{aligned} & \left\| \prod_{k=t}^{\tau} F + \nabla f_k(x_t^{(k-t)}, u_t^{(k-t)})[I, -K] \right\| \\ & \leq \sum_{k=t}^{\tau+1} \left\| F^{\tau+1-k} \sum_{S \subseteq \{t, \dots, \tau\}, |S|=k-t} \prod_{s \in S} \nabla f_s(x_t^{(s-t)}, u_t^{(s-t)})[I, -K] \right\| \\ & \leq \sum_{k=t}^{\tau+1} C_F \rho^{\tau+1-k} \sum_{S \subseteq \{t, \dots, \tau\}, |S|=k-t} \prod_{s \in S} \left\| \nabla f_s(x_t^{(s-t)}, u_t^{(s-t)})[I, -K] \right\|. \end{aligned}$$

Since the residual functions are Lipschitz continuous as in Assumption 1, their Jacobians satisfy $\|\nabla f_s(x_t^{(s-t)}, u_t^{(s-t)})\| \leq C_\ell$ for any $x_t^{(s-t)}$ and $u_t^{(s-t)}$. Letting $\bar{C} := C_\ell(1 + \|K\|)$, we get

$$\begin{aligned} & \left\| \prod_{k=t}^{\tau} F + \nabla f_k(x_t^{(k-t)}, u_t^{(k-t)})[I, -K] \right\| \\ & \leq \sum_{k=t}^{\tau+1} C_F \rho^{\tau+1-k} \sum_{S \subseteq \{t, \dots, \tau\}, |S|=k-t} \prod_{s \in S} \bar{C} = C_F (\rho + \bar{C})^{\tau+1-t}. \end{aligned} \quad (27)$$

Therefore, using (27),

$$\begin{aligned}
& \left\| \nabla f_\tau(x_t^{(\tau+1-t)}, u_t^{(\tau+1-t)})[I, -K] \prod_{k=t}^{\tau} F + \nabla f_k(x_t^{(k-t)}, u_t^{(k-t)})[I, -K] \right\| \\
& \leq \left\| \nabla f_\tau(x_t^{(\tau+1-t)}, u_t^{(\tau+1-t)})[I, -K] \right\| \left\| \prod_{k=t}^{\tau} F + \nabla f_k(x_t^{(k-t)}, u_t^{(k-t)})[I, -K] \right\| \\
& \leq C_F \bar{C} (\rho + \bar{C})^{\tau+1-t}.
\end{aligned} \tag{28}$$

Combing (27) and (28) with (26),

$$\begin{aligned}
\|\nabla g_t(x)\| & \leq \left\| \prod_{\tau=t}^{\infty} (F + \nabla f_\tau(x_t^{(\tau-t)}, u_t^{(\tau-t)})[I, -K])^\top g_\infty(0) \right\| \\
& + \underbrace{\left\| \sum_{\tau=t}^{\infty} \prod_{k=t}^{\tau} (F + \nabla f_k(x_t^{(k-t)}, u_t^{(k-t)})[I, -K])^\top 2F^\top P f_\tau(x_t^{(\tau-t)}, u_t^{(\tau-t)}) \right\|}_{(a)} \\
& + \underbrace{\left\| \sum_{\tau=t}^{\infty} \prod_{k=t}^{\tau} (F + \nabla f_k(x_t^{(k-t)}, u_t^{(k-t)})[I, -K])^\top 2(\nabla f_\tau(x_t^{(\tau-t)}, u_t^{(\tau-t)})[I, -K])^\top P x_t^{(\tau+1-t)} \right\|}_{(b)}.
\end{aligned}$$

Since $g_\infty(0) = 0$, the first term in the inequality above is 0. The second term satisfies

$$\begin{aligned}
(a) & \leq 2C_F C_\ell \|P\| \rho \sum_{\tau=t}^{\infty} (\rho + \bar{C})^{\tau+1-t} \|(x_t^{(\tau-t)}, u_t^{(\tau-t)})\| \\
& = 2C_F C_\ell \|P\| \rho \sum_{\tau=0}^{\infty} (\rho + \bar{C})^{\tau+1} \|x_t^{(\tau)}, u_t^{(\tau)}\| \\
& \leq 2C_F C_\ell \|P\| \rho \sqrt{\sum_{\tau=1}^{\infty} (\rho + \bar{C})^{2\tau}} \sqrt{\sum_{\tau=0}^{\infty} \|x_t^{(\tau)}\|^2 + \|u_t^{(\tau)}\|^2} \\
& \leq 2C_F C_\ell \|P\| \rho \sqrt{\frac{(\rho + \bar{C})^2}{1 - (\rho + \bar{C})^2}} \sqrt{\frac{C_F^2 \|Q + K^\top R K\|}{\min\{\lambda_{\min}(Q), \lambda_{\min}(R)\} (1 - (\rho + \bar{C})^2)}} \|x\|^2 \\
& = \frac{2C_F^2 \|P\| \rho C_\ell (\rho + \bar{C})}{1 - (\rho + \bar{C})^2} \sqrt{\frac{\|Q + K^\top R K\|}{\sigma}} \|x\|
\end{aligned} \tag{29}$$

where we have used the Cauchy to derive (29); $\lambda_{\min}(Q)$ and $\lambda_{\min}(R)$ are smallest eigenvalues of the matrices Q and R respectively and (30) follows from Assumption 2. Similarly, the third term satisfies

$$\begin{aligned}
(b) & \leq 2C_F \bar{C} \|P\| \sum_{\tau=t}^{\infty} (\rho + \bar{C})^{\tau+1-t} \|x_t^{(\tau+1-t)}\| \\
& \leq 2C_F \bar{C} \|P\| \sqrt{\sum_{\tau=1}^{\infty} (\rho + \bar{C})^{2\tau}} \sqrt{\sum_{\tau=1}^{\infty} \|x_t^{(\tau)}\|^2} \\
& \leq 2C_F \bar{C} \|P\| \sqrt{\frac{(\rho + \bar{C})^2}{1 - (\rho + \bar{C})^2}} \sqrt{\frac{C_F^2 \|Q + K^\top R K\|}{\lambda_{\min}(Q) (1 - (\rho + \bar{C})^2)}} \|x\|^2 \\
& \leq \frac{2C_F^2 \|P\| \bar{C} (\rho + \bar{C})}{1 - (\rho + \bar{C})^2} \sqrt{\frac{\|Q + K^\top R K\|}{\sigma}} \|x\|.
\end{aligned} \tag{31}$$

Putting (30) and (31) together, we conclude that

$$\|\nabla g_t(x)\| \leq \frac{2C_F^2\|P\|(\rho + \bar{C})(\rho C_\ell + \bar{C})}{1 - (\rho + \bar{C})^2} \sqrt{\frac{\|Q + K^\top RK\|}{\sigma}} \|x\| =: C_\nabla C_\ell \|x\|. \quad (32)$$

Rewriting (25) as

$$\begin{aligned} -v_t^* &= (R + B^\top PB)^{-1} x^\top F^\top P \nabla f_t(x, -Kx + v_t^*) [0, I] \\ &\quad + (R + B^\top PB)^{-1} B^\top P f_t(x, -Kx + v_t^*) \\ &\quad + (R + B^\top PB)^{-1} (v_t^*)^\top B^\top P \nabla f_t(x, -Kx + v_t^*) [0, I] \\ &\quad + (R + B^\top PB)^{-1} P f_t(x, -Kx + v_t^*) \nabla f_t(x, -Kx + v_t^*) [0, I] \\ &\quad + \frac{1}{2} (R + B^\top PB)^{-1} (B + \nabla f_t(x, -Kx + v_t^*) [0, I])^\top \nabla g_t(Fx + Bv + f_t(x, -Kx + v_t^*)) \end{aligned}$$

and taking the Euclidean norm on both sides, we obtain

$$\begin{aligned} \|v_t^*\| &\leq \left\| (R + B^\top PB)^{-1} x^\top F^\top P \nabla f_t(x, -Kx + v_t^*) [0, I] \right\| \\ &\quad + \left\| (R + B^\top PB)^{-1} B^\top P f_t(x, -Kx + v_t^*) \right\| \\ &\quad + \left\| (R + B^\top PB)^{-1} (v_t^*)^\top B^\top P \nabla f_t(x, -Kx + v_t^*) [0, I] \right\| \\ &\quad + \left\| (R + B^\top PB)^{-1} P f_t(x, -Kx + v_t^*) \nabla f_t(x, -Kx + v_t^*) [0, I] \right\| \\ &\quad + \left\| \frac{1}{2} (R + B^\top PB)^{-1} (B + \nabla f_t(x, -Kx + v_t^*) [0, I])^\top \right. \\ &\quad \quad \left. \nabla g_t(Fx + Bv + f_t(x, -Kx + v_t^*)) \right\| \\ &\leq \left\| R + B^\top PB \right\|^{-1} \left(C_\ell \|PF\| \|x\| + \bar{C} \left\| B^\top P \right\| \|x\| \right. \\ &\quad + 2C_\ell \left\| B^\top P \right\| \|v_t^*\| + \bar{C} \|P\| \|x\| + C_\ell \|P\| \|v_t^*\| \\ &\quad \left. + \frac{1}{2} C_\nabla C_\ell \|B + C_\ell I\| (\|F\| \|x\| + \|B\| \|v_t^*\| + \bar{C} \|x\| + C_\ell \|x\|) \right). \quad (33) \end{aligned}$$

Finally, assuming $C_\ell \leq \min \left\{ 1, \frac{\|R + B^\top PB\|}{4\|B^\top P\| + 2\|P\| + C_\nabla(\|B\| + 1)\|B\|} \right\}$, (33) yields

$$\|\pi_t^*(x) - \bar{\pi}(x)\| \leq C_\ell \|x\| \times \underbrace{\left(2\|R + B^\top PB\|^{-1} \left((\|PF\| + (1 + \|K\|)(\|PB\| + \|P\|)) + \frac{C_\nabla}{2} \|B + I\| (2 + \|F\| + \|K\|) \right) \right)}_{=: C_a^{\text{sys}}}$$

where the constant C_∇ is defined as

$$C_\nabla := \frac{2C_F^2\|P\|(\rho + \bar{C})(\rho + (1 + \|K\|))}{1 - (\rho + \bar{C})^2} \sqrt{\frac{\|Q + K^\top RK\|}{\sigma}}.$$

□

Theorem 5. Let $\gamma := (\rho + C_F C_\ell (1 + \|K\|))$. Suppose the black-box policy $\hat{\pi}$ is ε -consistent with the consistency constant ε satisfying $\varepsilon < \frac{1/C_F - C_a^{\text{sys}} C_\ell}{C_\ell + \|B\|}$. Suppose the Lipschitz constant C_ℓ satisfies $C_\ell < \min \{1, 1/(C_F C_a^{\text{sys}}), C_c^{\text{sys}}, (1 - \rho)/(C_F(1 + \|K\|))\}$. Let $(x_t : t \geq 0)$ denote a trajectory of states generated by the adaptive λ -confident policy $\pi_t = \lambda_t \hat{\pi} + (1 - \lambda_t) \bar{\pi}$ (Algorithm 1). Then it follows that π_t is an exponentially stabilizing policy such that $\|x_t\| \leq \frac{\gamma^t - \mu^t}{1 - \mu\gamma^{-1}} (C_F + \mu\gamma^{-1}) \|x_0\|$ for any $t \geq 0$ where $\mu := C_F (\varepsilon (C_\ell + \|B\|) + C_a^{\text{sys}} C_\ell)$.

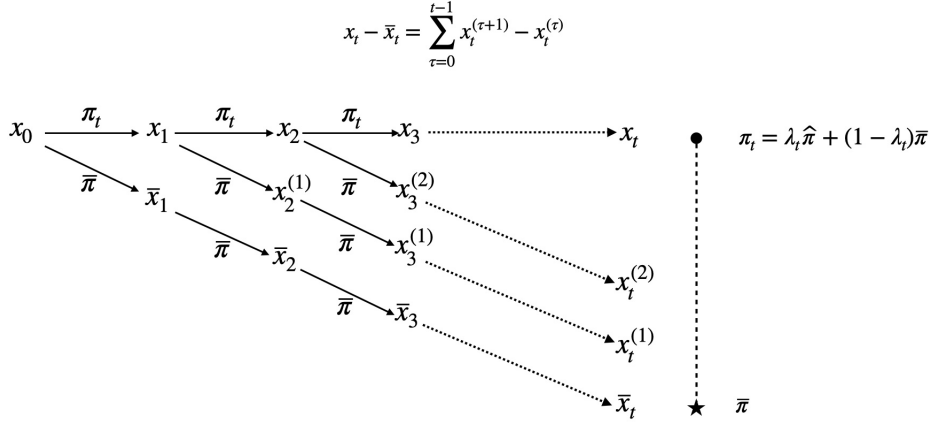


Figure 8: Telescoping sum of $x_t - x_t^*$.

Proof. We first introduce a new symbol $x_t^{(\tau)}$, which is the t -th state of a trajectory generated by the combined policy $\pi_t(x) = \lambda_t \hat{\pi}(x) + (1 - \lambda_t) \bar{\pi}(x)$ for the first τ steps and then switch to the model-based policy $\bar{\pi}$ for the remaining steps. Let $(\bar{x}_t : t \geq 0)$ be a trajectory of states generated by a model-based policy $\bar{\pi}$. As illustrated in Figure 1, for any $t \geq 0$,

$$x_t - \bar{x}_t = \sum_{\tau=0}^{t-1} x_t^{(\tau+1)} - x_t^{(\tau)}. \quad (34)$$

Let $(x_t : t \geq 0)$ and $(x'_t : t \geq 0)$ denote the trajectories of states at time t generated by the model-based policy $\hat{\pi}(x) = -Kx$ when the initial states are x_0 and x'_0 respectively. Then (21) leads to

$$x_t - x'_t = F^t(x_0 - x'_0) + \sum_{\tau=0}^{t-1} F^{t-1-\tau} (f_\tau(x_\tau, -Kx_\tau) - f_\tau(x'_\tau, -Kx'_\tau)),$$

yielding

$$\|x_t - x'_t\| \leq C_F \rho^t \left(\|x_0 - x'_0\| + C_\ell (1 + \|K\|) \sum_{\tau=0}^{t-1} \rho^{-1-\tau} \|x_\tau - x'_\tau\| \right)$$

where we have used the Lipschitz continuity of $(f_t : t \geq 0)$ and Assumption 2 so that $\|F^t\| \leq C_F \rho^t$ for any $t \geq 0$. The same argument as in Lemma 4 gives that for any $t \geq 0$,

$$\|x_t - x'_t\| \leq C_F (\rho + C_F \bar{C})^t \|x_0 - x'_0\|$$

where $\bar{C} := C_\ell (1 + \|K\|)$. Continuing from (34), $x_t - x_t^*$ can be represented by a telescoping sum (illustrated in Figure 8):

$$\|x_t - \bar{x}_t\| = \left\| \sum_{\tau=0}^{t-1} x_t^{(\tau+1)} - x_t^{(\tau)} \right\| \leq \sum_{\tau=0}^{t-1} \|x_t^{(\tau+1)} - x_t^{(\tau)}\| \leq \sum_{\tau=0}^{t-1} C_F \gamma^{t-\tau-1} \|x_{\tau+1}^{(\tau+1)} - x_{\tau+1}^{(\tau)}\|.$$

For any $t \geq 0$,

$$\begin{aligned} x_t^{(t)} - x_t^{(t-1)} &= x_t - x_t^{(t-1)} \\ &= (x_t - \lambda_t x'_t) + (\lambda_t x'_t - x_t^{(t-1)}) \\ &= \lambda_t (\hat{x}_t - x'_t) + (1 - \lambda_t) (\bar{x}_t - x_t^{(t-1)}) + \lambda_t (x'_t - x_t^{(t-1)}) \\ &= \lambda_t (\hat{x}_t - x'_t) + \lambda_t (x'_t - x_t^{(t-1)}) \end{aligned}$$

where x'_t , \widehat{x}_t and \bar{x}_t are the states generated by running an optimal policy π^* , a model-free policy $\widehat{\pi}$ and a model-based policy $\bar{\pi}$ respectively for one step with the same initial state x_{t-1} . Note that $x_t = \lambda_t \widehat{x}_t + (1 - \lambda_t) \bar{x}_t$ and $\bar{x}_t = x_t^{(t-1)}$. Therefore,

$$\lambda_t (\widehat{x}_t - x'_t) = \lambda_t \left(\underbrace{B(\widehat{\pi}(x_{t-1}) - \pi^*(x_{t-1}))}_{:= (a)} + \underbrace{f_{t-1}(x_{t-1}, \widehat{\pi}(x_{t-1})) - f_{t-1}(x_{t-1}, \pi^*(x_{t-1}))}_{:= (b)} \right).$$

For (a), we obtain the following bound:

$$\|(a)\| \leq \|B\| \|\widehat{\pi}(x_{t-1}) - \pi^*(x_{t-1})\| \leq \varepsilon \|B\| \|x_{t-1}\| \quad (35)$$

and (35) holds since the model-free policy $\widehat{\pi}$ is ε -consistent (Definition 1). Similarly, for (b), since the functions $(f_t : t \geq 0)$ are Lipschitz continuous (Assumption 1),

$$\|(b)\| \leq \varepsilon C_\ell \|x_{t-1}\|. \quad (36)$$

Applying Theorem 4, $\|x'_t - x_t^{(t-1)}\| \leq C_a^{\text{sys}} C_\ell \|x_{t-1}\|$. Combining (35) and (36) and applying Lemma 4, $\|x_t - \bar{x}_t\| \leq \mu \sum_{\tau=0}^{t-1} \gamma^{t-\tau-1} \|x_\tau\|$ where $\mu := C_F (\varepsilon (C_\ell + \|B\|) + C_a^{\text{sys}} C_\ell)$, therefore,

$$\frac{\|x_t\|}{\gamma^t} \leq \frac{1 - (\mu\gamma^{-1})^t}{1 - \mu\gamma^{-1}} (C_F + \mu\gamma^{-1}) \|x_0\|.$$

Hence, if $\mu < 1$, $\|x_t\| \leq \frac{\gamma^t - \mu^t}{1 - \mu\gamma^{-1}} (C_F + \mu\gamma^{-1}) \|x_0\|$, the linearly combined policy π_t is an exponentially stabilizing policy. \square

E.2 Proof of Theorem 2

To show the stability results, noting that the policy is switched to the model-based policy after $t \geq t_0$. Since the Lipschitz constant C_ℓ satisfies $C_\ell < \frac{1-\rho}{C_F(1+\|K\|)}$ where $\|F^t\| \leq C_F \rho^t$ for any $t \geq 0$, then the model-based policy $\bar{\pi}$ is exponentially stable as shown in Lemma 4. Let $\mu := C_F (\varepsilon (C_\ell + \|B\|) + C_a^{\text{sys}} C_\ell)$ and $\gamma := \rho + C_F C_\ell (1 + \|K\|) < 1$. Applying Theorem 5 and Lemma 4, for any $t \geq 0$,

$$\|x_t\| \leq \frac{\mu^{t_0}}{\mu\gamma^{-1} - 1} (C_F + \mu\gamma^{-1}) (\rho + C_F C_\ell (1 + \|K\|))^{t-t_0} \|x_0\|.$$

Since $\lambda_{t+1} < \lambda_t - \alpha$ for all $t \geq 0$ with some $\alpha > 0$, t_0 is finite and the adaptive λ -confident policy is an exponentially stabilizing policy.

F Competitive Ratio Analysis

F.1 Proof of Theorem 3

Before proceeding to the proof of Theorem 3, we prove the following lemma that will be useful.

Lemma 5. *Suppose $\varepsilon \leq \lambda_{\min}(Q)/(2\|H\|)$. If the adaptive λ -confident policy $\pi_t = \lambda_t \widehat{\pi} + (1 - \lambda_t) \bar{\pi}$ (Algorithm 1) is an exponentially stabilizing policy, then the competitive ratio of the linearly combined policy is $\text{CR}(\varepsilon) = O((1 - \lambda) \overline{\text{CR}}_{\text{model}}) + O\left(1 / \left(1 - \frac{2\|H\|}{\sigma} \varepsilon\right)\right) + O(C_\ell \|x_0\|)$.*

Proof of Lemma 5. Let $H := R + B^\top P B$. Fix any sequence of residual functions $(f_t : t \geq 0)$. Denote by $f_t := f_t(x_t, u_t)$, $f_t^* := f_t(x_t^*, u_t^*)$ and x_t^* and u_t^* the offline optimal state and action at time

t . With $u_t = \lambda_t \hat{u}_t + (1 - \lambda_t) \bar{u}_t$ at each time t , Lemma 2 implies that the *dynamic regret* can be bounded by

$$\begin{aligned}
\text{DynamicRegret} &:= \text{ALG} - \text{OPT} \leq \sum_{t=0}^{\infty} \eta_t^\top H \eta_t + O(1) \\
&+ 2 \sum_{t=0}^{\infty} \eta_t^\top B^\top \left(\sum_{\tau=t}^{\infty} (F^\top)^\tau P (f_{t+\tau} - f_{t+\tau}^*) \right) \\
&+ \sum_{t=0}^{\infty} (f_t^\top P f_t - (f_t^*)^\top P f_t^*) + 2x_0^\top \left(\sum_{t=0}^{\infty} (F^\top)^{t+1} P (f_t - f_t^*) \right) \\
&+ 2 \sum_{t=0}^{\infty} \left(f_t^\top \sum_{\tau=0}^{\infty} (F^\top)^{\tau+1} P f_{t+\tau+1} - (f_t^*)^\top \sum_{\tau=0}^{\infty} (F^\top)^{\tau+1} P (f_{t+\tau+1}^*) \right) \\
&+ 2 \sum_{t=0}^{\infty} \left(\sum_{\tau=t}^{\infty} (F^\top)^\tau P f_{t+\tau}^* \right) B H^{-1} B^\top \left(\sum_{\tau=t}^{\infty} (F^\top)^\tau P (f_{t+\tau}^* - f_{t+\tau}) \right). \quad (37)
\end{aligned}$$

Consider the auxiliary linear policy defined in (12). Provided with any state $x \in \mathbb{R}^n$, the linearly combined policy π_t is given by

$$\pi_t(x) = \lambda_t \hat{\pi}(x) + (1 - \lambda_t) \bar{\pi}(x) = \pi'(x) + \lambda_t (\hat{\pi}(x) - \pi'(x)) + (1 - \lambda_t) (\bar{\pi}(x) - \pi'(x)),$$

implying $\eta_t = \lambda_t (\hat{\pi}(x_t) - \pi'(x_t)) + (1 - \lambda_t) (\bar{\pi}(x_t) - \pi'(x_t))$ in (37). Moreover, $\sum_{t=0}^{\infty} \eta_t^\top H \eta_t \leq \sum_{t=0}^{\infty} \|H\| \|\eta_t\|^2$, therefore, denoting by $\lambda := \lim_{t \rightarrow \infty} \lambda_t$,

$$\sum_{t=0}^{\infty} \eta_t^\top H \eta_t \leq 2 \|H\| \left(\sum_{t=0}^{\infty} \|\hat{\pi}(x_t) - \pi'(x_t)\|^2 + (1 - \lambda) \sum_{t=0}^{\infty} \|\bar{\pi}(x_t) - \pi'(x_t)\|^2 \right), \quad (38)$$

where in (38) we have used the Cauchy–Schwarz inequality. Since the model-free policy $\hat{\pi}$ is ε -consistent, it follows that

$$\begin{aligned}
\|\hat{\pi}(x_t) - \pi'(x_t)\|^2 &\leq 2 \|\pi_t^*(x_t) - \pi'(x_t)\|^2 + 2 \|\hat{\pi}(x_t) - \pi_t^*(x_t)\|^2 \\
&\leq 2 \|\pi_t^*(x_t) - \pi'(x_t)\|^2 + 2\varepsilon \|x_t\|^2.
\end{aligned}$$

Furthermore, since the cost OPT' induced by the auxiliary linear policy (12) is smaller than OPT ,

$$\sum_{t=0}^{\infty} \|\pi_t^*(x_t) - \pi'(x_t)\|^2 \leq \frac{\text{OPT} + \text{OPT}'}{\lambda_{\min}(R)} \leq \frac{2\text{OPT}}{\lambda_{\min}(R)} \quad (39)$$

where $\lambda_{\min}(R) > 0$ denotes the smallest eigenvalue of $R \succ 0$.

The linear quadratic regulator is $\bar{\pi}(x) = -Kx = -(R + B^\top P B)^{-1} B^\top P A x$ for a given state $x \in \mathbb{R}^n$, we have for all $t \geq 0$,

$$\|\bar{\pi}(x_t) - \pi'(x_t)\|^2 = \left\| \sum_{\tau=t}^{\infty} (F^\top)^{\tau-t} P f_\tau^* \right\|^2. \quad (40)$$

Plugging (39) and (40) into (38),

$$\sum_{t=0}^{\infty} \eta_t^\top H \eta_t \leq 2 \|H\| \left(\left(\frac{2\text{OPT}}{\lambda_{\min}(R)} + \varepsilon \sum_{t=0}^{\infty} \|x_t\|^2 \right) + \sum_{t=0}^{\infty} \left\| \sum_{\tau=t}^{\infty} (F^\top)^{\tau-t} P f_\tau^* \right\|^2 \right). \quad (41)$$

The algorithm cost ALG can be bounded by $\text{ALG} \geq \sum_{t=0}^{\infty} x_t^\top Q x_t + u_t^\top R u_t \geq \sum_{t=0}^{\infty} \lambda_{\min}(Q) \|x_t\|^2$, therefore, (41) leads to

$$\sum_{t=0}^{\infty} \eta_t^\top H \eta_t \leq 2 \|H\| \left(\left(\frac{2\text{OPT}}{\lambda_{\min}(R)} + \varepsilon \frac{\text{ALG}}{\lambda_{\min}(Q)} \right) + \sum_{t=0}^{\infty} \left\| \sum_{\tau=t}^{\infty} (F^\top)^{\tau-t} P f_\tau^* \right\|^2 \right). \quad (42)$$

Moreover, we have the following lemma holds.

Lemma 6. *The optimal cost OPT can be bounded from below by*

$$\text{OPT} \geq \frac{D_0(1-\rho)^2}{C_F^2 \|P\|^2} \sum_{t=0}^{\infty} \left\| \sum_{\tau=t}^{\infty} (F^\top)^{\tau-t} P f_\tau^* \right\|^2.$$

Proof of Lemma 6. the optimal cost can be bounded from below by

$$\begin{aligned} \text{OPT} &= \sum_{t=0}^{\infty} (x_t^*)^\top Q x_t^* + (u_t^*)^\top R u_t^* \\ &\geq \sum_{t=0}^{\infty} \lambda_{\min}(Q) \|x_t^*\|^2 + \lambda_{\min}(R) \|u_t^*\|^2 \\ &\geq 2D_0 \sum_{t=0}^{\infty} (\|A x_t^*\|^2 + \|B u_t^*\|^2) + \frac{1}{2} \sum_{t=0}^{\infty} \lambda_{\min}(Q) \|x_t^*\|^2 \\ &\geq D_0 \sum_{t=0}^{\infty} \|A x_t^* + B u_t^*\|^2 + \frac{1}{2} \sum_{t=0}^{\infty} \lambda_{\min}(Q) \|x_t^*\|^2. \end{aligned} \quad (43)$$

Since $x_{t+1}^* = A x_t^* + B u_t^* + f_t^*$ for all $t \geq 0$,

$$\begin{aligned} \text{OPT} &\geq D_0 \sum_{t=0}^{\infty} \|x_{t+1}^* - f_t^*\|^2 + \frac{1}{2} \sum_{t=0}^{\infty} \lambda_{\min}(Q) \|x_t^*\|^2 \\ &\geq \frac{D_0}{2} \sum_{t=0}^{\infty} \|f_t^*\|^2 + \left(\frac{\lambda_{\min}(Q)}{2} - D_0 \right) \sum_{t=0}^{\infty} \|x_t^*\|^2 \end{aligned} \quad (44)$$

for some constant $D_0 := \min\left\{ \frac{\lambda_{\min}(R)}{\|B\|}, \frac{\lambda_{\min}(Q)}{2\|A\|}, \frac{\lambda_{\min}(Q)}{2} \right\} \geq \frac{\sigma}{\max\{2, \|A\|, \|B\|\}}$ (Assumption 2) that depends on known system parameters A, B, Q and R where in (43), $\lambda_{\min}(Q)$, $\lambda_{\min}(R)$ are the smallest eigenvalues of positive definite matrices Q, R , respectively. Let $\psi_t := \sum_{\tau=t}^{\infty} (F^\top)^\tau P f_{t+\tau}^*$ for all $t \geq 0$. Note that $F = A - BK$ and we define $\rho := (1 + \rho(F))/2 < 1$ where $\rho(F)$ denotes the spectral radius of F . From the Gelfand's formula, there exists a constant $C_F \geq 0$ such that $\|F^t\| \leq C_F \rho^t$ for all $t \geq 0$. Therefore,

$$\begin{aligned} \sum_{t=0}^{\infty} \|\psi_t\|^2 &:= \sum_{t=0}^{\infty} \left\| \sum_{\tau=t}^{\infty} (F^\top)^\tau P f_{t+\tau}^* \right\|^2 \leq C_F^2 \|P\|^2 \sum_{t=0}^{\infty} \left(\sum_{\tau=t}^{\infty} \rho^\tau \|f_{t+\tau}^*\| \right)^2 \\ &= C_F^2 \|P\|^2 \sum_{t=0}^{\infty} \sum_{\tau=t}^{\infty} \sum_{\ell=0}^{\infty} \rho^\tau \rho^\ell \|f_{t+\tau}^*\| \|f_{t+\ell}^*\| \\ &\leq \frac{C_F^2}{2} \|P\|^2 \sum_{t=0}^{\infty} \sum_{\tau=t}^{\infty} \sum_{\ell=0}^{\infty} \rho^\tau \rho^\ell \left(\|f_{t+\tau}^*\|^2 + \|f_{t+\ell}^*\|^2 \right). \end{aligned} \quad (45)$$

Continuing from (45),

$$\begin{aligned}
\sum_{t=0}^{\infty} \|\psi_t\|^2 &\leq \frac{C_F^2}{2} \|P\|^2 \left(\sum_{\ell=0}^{\infty} \rho^\ell \right) \sum_{t=0}^{\infty} \sum_{\tau=t}^{\infty} \rho^\tau \|f_{t+\tau}^*\|^2 + \frac{C_F^2}{2} \|P\|^2 \left(\sum_{\tau=t}^{\infty} \rho^\tau \right) \sum_{t=0}^{\infty} \sum_{\ell=0}^{\infty} \rho^\ell \|f_{t+\ell}^*\|^2 \\
&\leq \frac{C_F^2}{1-\rho} \|P\|^2 \sum_{t=0}^{\infty} \sum_{\tau=t}^{\infty} \rho^\tau \|f_{t+\tau}^*\|^2 \leq \frac{C_F^2}{1-\rho} \|P\|^2 \sum_{t=0}^{\infty} \sum_{\tau=0}^{\infty} \rho^\tau \|f_{t+\tau}^*\|^2 \\
&= \frac{C_F^2}{1-\rho} \|P\|^2 \left(\sum_{\tau=0}^{\infty} \rho^\tau \right) \left(\sum_{t=0}^{\infty} \|f_t^*\|^2 \right) \\
&\leq \frac{C_F^2}{(1-\rho)^2} \|P\|^2 \sum_{t=0}^{\infty} \|f_t^*\|^2. \tag{46}
\end{aligned}$$

Putting (46) into (44), we obtain $\text{OPT} \geq \frac{D_0(1-\rho)^2}{C_F^2\|P\|^2} \sum_{t=0}^{\infty} \|\psi_t\|^2$. \square

Combining Lemma 6 with (42),

$$\sum_{t=0}^{\infty} \eta_t^\top H \eta_t \leq 2\|H\| \left(\frac{2\text{OPT}}{\lambda_{\min}(R)} + \varepsilon \frac{\text{ALG}}{\lambda_{\min}(Q)} + (1-\lambda) \frac{C_F^2\|P\|^2\text{OPT}}{D_0(1-\rho)^2} \right). \tag{47}$$

Furthermore, since P is symmetric, $f_t^\top P f_t - (f_t^*)^\top P f_t^* = (f_t + f_t^*)^\top P (f_t - f_t^*)$, the RHS of the inequality (37) can be bounded by

$$\begin{aligned}
&\sum_{t=0}^{\infty} \eta_t^\top H \eta_t + 2 \sum_{t=0}^{\infty} \left(\|B\eta\| \left\| \sum_{\tau=t}^{\infty} (F^\top)^\tau P (f_{t+\tau} - f_{t+\tau}^*) \right\| + \|P(f_t + f_t^*)\| \|f_t - f_t^*\| \right. \\
&\quad + \|x_0\| \left\| \sum_{t=0}^{\infty} (F^\top)^{t+1} P (f_t - f_t^*) \right\| + \|f_t\| \left\| \sum_{\tau=0}^{\infty} (F^\top)^{\tau+1} P (f_{t+\tau+1} - f_{t+\tau+1}^*) \right\| \\
&\quad + \left\| \sum_{\tau=0}^{\infty} (F^\top)^{\tau+1} P f_{t+\tau+1}^* \right\| \|f_t^* - f_t\| \\
&\quad \left. + \|BH^{-1}B^\top\| \left\| \sum_{\tau=t}^{\infty} (F^\top)^\tau P f_{t+\tau}^* \right\| \left\| \sum_{\tau=t}^{\infty} (F^\top)^\tau P (f_{t+\tau}^* - f_{t+\tau}) \right\| \right).
\end{aligned}$$

Furthermore, by our assumption, the linearly combined policy π is an exponentially stabilizing policy and since f_t is Lipschitz continuous with a Lipschitz constant C_ℓ , using (47) and noting that $\text{OPT} > 0$,

$$\begin{aligned}
\text{ALG} - \text{OPT} &\leq 2\|H\| \left(\frac{1}{\sigma} (2\text{OPT} + \varepsilon\text{ALG}) + (1-\lambda) \frac{C_F^2\|P\|^2 \max\{2, \|A\|, \|B\|\} \text{OPT}}{\sigma(1-\rho)^2} \right) \\
&\quad + O(C_\ell \|x_0\|).
\end{aligned}$$

Rearranging the terms gives the competitive ratio bound in Lemma 5. \square

Now, applying Lemma 5, we complete our competitive analysis by proving Theorem 3.

Proof of Theorem 3. Continuing from Theorem 5, it shows that if the Lipschitz constant C_ℓ satisfies $C_\ell < \frac{1-\rho}{C_F(1+\|K\|)}$ where $\|F^t\| \leq C_F \rho^t$ for any $t \geq 0$ and the consistency error ε satisfies $\varepsilon < \min \left\{ \frac{\sigma}{2\|H\|}, \frac{1/C_F - C_a^{\text{sys}} C_\ell}{C_\ell + \|B\|} \right\}$ where C_a^{sys} is defined in (7), then

$$\|x_t\| \leq \frac{\gamma^t - \mu^t}{1 - \mu\gamma^{-1}} (C_F + \mu\gamma^{-1}) \|x_0\|,$$

for all $t \geq 0$ with some $\mu < 1$. Therefore, Lemma 5 implies Theorem 3. \square